공학박사학위논문

Study of Unique Morphological Features of Primo Vascular System

프리모 시스템의 독특한 형태학적 특징 분석 연구

2017년 8월

서울대학교 융합과학기술대학원

융합과학부 나노융합전공

Sharon Jiyoon Jung (정 지 윤)

공학박사학위논문

Study of Unique Morphological Features of Primo Vascular System

프리모 시스템의 독특한 형태학적 특징 분석 연구

2017년 8월

서울대학교 융합과학기술대학원

융합과학부 나노융합전공

Sharon Jiyoon Jung (정 지 윤)

Study of Unique Morphological Features of Primo Vascular System

Sharon Jiyoon Jung

Supervised by
Professor Yoon-Kyu Song

A Dissertation in Nano science and technology
Submitted to the Faculties of Seoul National University
in Partial Fulfillment of the Requirements for the Degree of
Doctor of Philosophy

August 2017

Department of Transdisciplinary,
Program in Nano Science and Technology
The Graduate School of Convergence Science and Technology
Seoul National University

Study of Unique Morphological Features of Primo Vascular System

지도교수 송 윤 규

이 논문을 공학박사 학위논문으로 제출함

2017년 8월

서울대학교 융합과학기술대학원

융합과학부 나노융합전공

Sharon Jiyoon Jung (정 지 윤)

정지윤의 공학박사 학위논문을 인준함

2017년 8월

위 원 장 김 연 상 (인)

부위원장 송 윤 규 (인)

위 원 소 광 섭 (인)

위 원 류 판 동 (인)

위 원 김 성 철 (인)

Abstract

Acupuncture has been a major medical practice for thousands of years in China, Korea, and Japan, yet the mechanism underlying acupuncture has still not been unambiguously identified on a scientific basis.

From the many previous studies, the known anatomical structure corresponding to the classical acupuncture points and meridians has been presented as the Primo Vascular System (PVS), which was first discovered by Bong Han Kim in early1960. It is being introduced in public as a newly-discovered third circulatory system on par with the circulatory and lymphatic system.

Despite its potential importance in health-related fields, it has been ignored for a long time. Only recently, researchers have been carrying out a lot of well-designed research studies to investigate its physical and physiological peculiarity of acupuncture system based on the anatomical and scientific bases, but still it has not been identified fully enough. And even results achieved from experiments performed under the Kim's theory; there has been a lot of controversy issue over its reliability.

Thus, in this thesis, the three hypotheses on PVS theory were mainly focused to prove for its distinguishing features and at the same time, suggest a new analysis method to make us to understand the complexity of this system from a new perspective.

First, in order to PVS accepted as a liquid flowing system, there have always been two major issues coming up. The first one was directly to show the flow of liquid in PVS and the second was to

explain why it was not observed in the conventional histological analysis of animal tissues. In order to find the answers to those, we injected fluorescent nanoparticles (FNPs) into a primo node and traced them along primo vessels which was located in the inside a fat tissue which is parallel to the linea alba in the parietal side of the abdominal wall. In previous experiment, the simple flow of injected staining dye (alcian blue) was observed. However, in this experiment, we could possibly trace the flow of FNPs to other subsystems of the PVS. Not just that in this work, we could give a small clue as to why PVS was difficult to observe in conventional histology.

In our previous work**,** we proposed the importance for finding an effective method to find the PVS in skin and need for study on the ultrastructure of the primo vessel (PV). So, in following chapters, we investigated the detailed morphological features of PV inside a lymph vessel with a transmission electron microscope (TEM) and compared the results with the previous study of the PV found on the surfaces of internal organs. These data confirm that the subsystem of PV is found in different parts of body revealed the similarity to one another.

Lastly, we focused on explaining the newly developed analysis methods of the acupuncture points (APs) located in the skin of the mouse. In several studies, many of them were still described between MCs and APs; however, they did not provide the answer for the reason.

By studying the mast cells (MCs) distribution and densities of the whole mouse ventral skin, we used this information to infer the locations, sizes and depths of the skin layers of APs. This type of estimation was done first time.

The methods used in this study can be useful to investigate further gross anatomical features of APs. Also, due to the significant roles of MCs in our body, it is clearly implied that acupuncture plays an

important role in MCs in the treatment of diseases. By having the more precise knowledge of skin AP locations and sizes to submillimeter precision, along with their cytological characterizations, would provide significant contributions to both scientific investigations and further acupuncture treatment.

Key words: Primo Vascular System, Mast Cell, Toluidine blue, Protocol, Acupuncture point, Meridian, Immune Systems, Transmission Electronic microscope.

Student Number: 2014-30808

Table of Contents

Abstract…….... **I**

Table of Contents……..……..……... **II**

List of Figures and Tables .....……..... **III**

Chapter 1. Introduction

1.1 A history of PVS research……..... **1**

1.2 PVS's characteristics and its relations with other circulation…... **5**

References……. **12**

Chapter 2. Observation of a Flowing Duct in the Abdominal Wall by Using Nanoparticles

2.1 Introduction……... **15**

2.2 Material & Methods……. **17**

2.2.1 Animal preparation……..... **17**

2.2.2 Injection and observation of fluorescent nanoparticles.... **18**

2.2.3 Histological Analysis……..... **19**

2.3 Results……..... **20**

2.4 Discussion……. **24**

Reference……..... **27**

Chapter 3. Ultrastructure of a Mobile Threadlike Tissue Floating in a Lymph Vessel

3.1 Introduction…….…… **29**

3.2 Materials & Methods……..…….….... **30**

3.2.1 Animal Preparation……..... **30**

3.2.2 Visualization and Observation of the PVS…… **30**

3.3 Results…….…… **32**

3.4 Discussion……. **36**

References…….….. **38**

Chapter 4. Study of Skin Primo Vascular System

4.1 Superficial Primo Node (S-PN) Study…… **41**

4.1.1 Introduction…… **41**

4.1.2 Materials & Methods…….. **45**

4.1.3 Results…… **47**

References……... **52**

4.2 Ogay Primo Node Study……... **54**

References……... **62**

4.3 Distribution of Mast Cells and Locations, Depths, and Sizes of the Putative Acupoints CV 8 and KI 16……... **64**

4.3.1 Introduction…… **64**

4.3.2 Materials & Methods……..... **67**

4.3.3 Results…… **72**

4.3.4 Discussion…….. **78**

References……... **82**

Chapter 5. Further study

5.1 Skin Chromaffin Cell Study…….. **85**

5.1.1 Introduction…… **85**

5.1.2 Materials & Methods…….. **89**

References……... **93**

5.2 Medical Application in PVS……. **95**

References……... **100**

Chapter 6. Conclusion…….. **103**

국문 초록……. **106**

감사의 글…… **111**

List of Figures and Tables

Figure 1.1	Weblike network of BHDs …….....	**4**
Figure 1.2	A diagram of three types of circulatory system……	**5**
Figure 1.3	A schematic drawing of PVS……..…….	**6**
Figure 1.4	Structural properties of primo sub-vessel and of blood and lymphatic capillary……	**7**
Figure 1.5	Comparison of the fluorescent staining in PV, Vascular and Lymphatic vessels……	**8**
Figure 1.6	Composition of the resident immune related cells in PN…….	**9**
Figure 1.7	Morphological studies of PV isolated from lymphatic vessels……...	**10**
Figure 2.1	The anatomical position of the novel flowing duct in the abdominal wall fat band…..……..	**16**
Figure 2.2	Phase contrast microscope images of the PVS……	**21**
Figure 2.3	Histological analysis of the PV, peritoneum and fascia……...	**23**
Figure 2.4	Mast cells in the PN…….....	**25**
Figure 3.1	Stereomicroscopic images of lymph ducts in which a PVS was stained with alcian blue…….	**32**
Figure 3.2	Images of a harvested lymph duct in which a PV was stained with alcian blue…….....	**33**
Figure 3.3	Cross-sectional images of a PV in the harvested lymph duct……..	**35**
Figure 4.1.1	Longitudinal section of S-PN showing the histological structure…….....	**42**
Figure 4.1.2	An image of smooth muscle fiber radiating towards connective tissue……	**43**
Figure 4.1.3	An image of inner substance of S- PN…….	**43**
Figure 4.1.4	An acupoint /meridian map of a mouse…….....	**45**
Figure 4.1.5	Descriptive picture of the sample block preparation…….....	**47**
Figure 4.1.6	Putative S-PN found on CV8…….....	**49**
Figure 4.1.7	Analysis of cells founded in the putative S-PV on CV8 location.	**50**
Figure 4.2.1	Morphology and anatomical distribution of the neurovascular bundles (NBs)…….....	**54**
Figure 4.2.2	Relationship of the neurovascular bundles (NBs) and the acupuncture points (APs)……..	**56**

Figure 4.2.3	Schematic diagram showing the distance of putative APs and Okay node…….	**56**
Figure 4.2.4	Illustration of neurovascular plexuses of coiled blood vessels……...	**58**
Figure 4.2.5	Images showing the anatomical location of ogay nodes…..……	**59**
Figure 4.3.1	The schematic illustration of acupoints along the meridian in the abdomen of a mouse……..	**68**
Figure 4.3.2	Cross-sectional images of a mouse abdomen showing its layers…….	**69**
Figure 4.3.3	A toluidine-blue stained cross sectioned sample……..	**69**
Figure 4.3.4	Graphical representation of MC density ……..	**73**
Figure 4.3.5	The image of the selected five regions of high density of MCS with ellipses……..	**74**
Figure 4.3.6	A magnified view of the region of CV 8……..	**74**
Figure 4.3.7	An H&E image showing the fat pad under the abdominal wall muscle……...	**77**
Figure 4.3.8	A magnified view of the MC populated Area…….....	**78**
Figure 5.1.1	Chromaffin cells detected in sinus……	**87**
Figure 5.1.2	Electron micrograph of the sinus of superficial primo node…..…	**87**
Figure 5.1.3	Electron micrograph showing chromaffin cells……	**88**
Figure 5.1.4	The color chart of cells by different staining methods…….	**91**

List of Table

Table 4.1.1	A summary table of substances can be found in S-PN…….	**44**
Table 4.3.1	Number density of mast cells at the putative acupoints CV8 and two KI16 and at the fat pad…….	**75**
Table 4.3.2	Locations, depths, and sizes of the putative acupoints CV8 and two KI16……..	**76**

Chapter 1

Introduction

1.1 A brief history of PVS research

1.2 PVS's characteristics and its relations with other circulation

Chapter 1

This chapter briefly outlines the general introduction of primo vascular system (PVS) and the existence and function of PVS.

1.1 A Brief History of the PVS research

In this part, a short history of the PVS is presented. This work, it was named Bong-Han Theory after the developer, Bong-Han Kim. The most of his work was happened in the Kyung-Rak Research Institute of North Korea (KRI) in early 1960s.

Bong-Han Kim was born in 1916 and graduated from the College of Medicine Seoul National University in 1941. He was an associate professor at Pyung Yang Medical School, Physiology Lab., when he introduced his founding [1]. His entire discovery was made sometime between 1962 and 1965, when he was the director of the institute (KRI). This institute was known to be a National Institute of North Korea and maybe established around this period [1]. The North Korean government supported Kim's research by supplying his team with various analytical instruments such as

microscopes and radioactive tracers, most of which were imported from Eastern Europe [26]. He was awarded the People's Prize for his work on 2 February 1962 [27].

His five publications were the collective works of his members in this place. While working as director of North Korea's Kyung-Rak institute (KRI) from 1962 to 1965, Kim published five articles in the *Journal of Jo Sun Medicine*, about acupuncture, the Kyungrak system, and the "Sanal" theory. These articles form the basis of the proposed primo-vascular system, which attracted some interest as late as in the early 2010s [1, 2]. However, oddly enough these articles, there was no descriptions of the method or material section at all.

Among the series of five, in the second article he mentioned that he found the most important material which corresponding to acupuncture points and meridians for the first time. Thereafter his team found the Bong-Han network which was extended throughout an animal's body. This second copy was translated into English and distributed to worldwide libraries [1].

The third article was published after the second and it was about a systematic investigation of the new circulatory system. The fourth and fifth were announced in 1965 and mostly, the last two articles were about the "SANAL", which we now called the primo microcell (0.8 um ~2.4um in size) and functioning like the embryonic-like stem cells. Despite the fact that he and his team introduced the meaningful discoveries in the world, for some unknown reasons, the KRI was closed in 1966, and they simply disappeared without a trace. Until the present time, we could not get the evidence of his fate and only the rumors were flying around.

Many researchers from countries including Russia, China, and Japan showed the interest of this subject in 1963 and many teams attempted to repeat his result. However, there was no record that they succeeded in their trial to reproduce Bong-Han Kim's work. Due to their failure, many researchers become skeptics about his work and stepped away from the earliest impressionist interest.

At that time, only one Japanese researcher, Satoru Fujiwara, who was an assistant professor of anatomy at Osaka City University, was stubborn enough to continue this work to observe this mysterious system in blood vessels and on the organ surface of rabbits [1]. Even though there were many questions remained, but with his own techniques, he observed the a few subsystems of Bong-Han Kim's findings. However, for the many trials have done during this six months period, he could not figure out a hint of blue dying agent. Based on his observation, he wrote one journal article in 1967 and published a book, "Discovery of Acupuncture Meridian" in Japanese. But people in Japan became skeptical of his result after Kim was disappeared in North Korea and such a social atmosphere, he could not continue this research.

It seemed to be Bong-Han Kim's work was buried underground and forgotten from people's memory. In the year of 2002, Jiowen Jiang from the Chinese veterinary student begins a trial experiment to prove Kim's claim on the existence of new circulatory system and in that summer, Jiang's team was able to find intravascular Bong-Han vessels from the rabbits, which was the restart of PVS research [1]. Professor Kwang-Sup Soh visited him in china and decided to continue this work in his laboratory in SNU in 2002. In the year of 2010, the name of Bong-Han Theory was changed to Primo Vascular System (PVS) theory for the call it easy.

For the first half year after his team started, they faced many failures and around six months passed, his team could observe for the first time. However, his team was hard to reproduce of their work and around this time, professor Soh looked for professor Fujiwara and finally visited in Japan. Professor Fujiwara showed his work in film to Professor Soh and gave his recorded notes which was his experimental procedures were written [1].

After professor Soh came back to Korea, his team put all the efforts to observe the PVS which was known to be extending throughout the animal's body. With some major breakthroughs, the striking progress was reported through his team with detection techniques developed by SNU team (fig 1.1. A, B & C). And at the same time, many research teams were emerging from

countries. This was the second phase of the PVS research began and its efforts continued to look for a complete PVS.

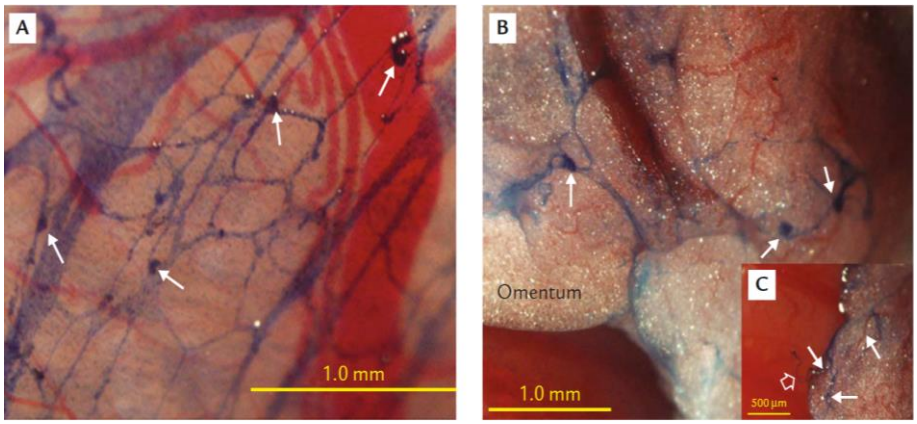

Fig.1.1 **Weblike network of BHDs revealed by using trypan blue**

(A) Web of BHDs on visceral peritoneum around stomach near rat spleen; several small BHCs at crossing points (arrows); blood capillaries not stained. **(B)** Network of BHDs on omentum below stomach and over small intestime; three small corpuscles at crossing points of BHDs (arrows). **(C)** Inset: another part of same omentum as (A); floating BHD (open arrow) connected to BHDs (arrows) in omentum, showing BHDs on omentum as poart of larger network of freely movable BHDs on internal organ surfaces. (*Microsc Res Tech 2007; 70: 34−43*)

1.2 PVS's characteristics and its relations with other circulation systems

As described in the history section, the primo-vascular system (PVS) was first reported in the early 1960s by Bong Han Kim. It was a newly described circulatory system in addition to the well-known blood and lymphatic system as shown in fig 1.2. That is why it was introduced as third circulatory system in public.

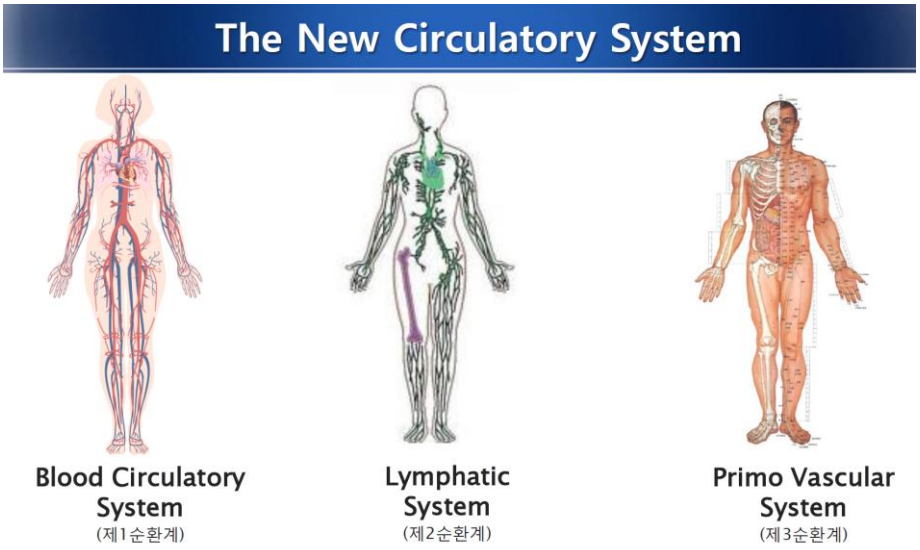

Fig.1.2. **A diagram of three types of circulatory system including primo vascular system. (PVS)**

Dr. Kim published a series of five reports on the anatomical structure and physiological study of Acupuncture Points (APs) and Acupuncture Meridians (AMs) [20-23] and he stated that PNs and PVs correspond to APs and AMs [19]. The linkage of PVs forms a circulatory system. One of reviewer named Chan emphasized the mentioned studies of gross anatomical correlations, biophysical approaches, including the electrical properties and physiological measurements in this field [3].

The PVS is extended throughout whole body and forms a network as other system do. Founder Kim was claimed [19] that this system corresponded

with the acupuncture meridians of human and mammals. This circulation system serves the role as meridians in acupuncture but it has not been proven yet [4]. To be more specific, the PVS can be found in the various sites in the body. Depends on the location we found, we called name differently. The figure 1.3 below clearly showed this classification. PVS can be categorized as (1) an intravascular PVS that runs along the interior of the large veins, arteries, and lymphatic vessels and is afloat in the blood/lymph stream, (2) a superficial PVS located in the skin, (3) an organ-surface PVS that spreads on various internal organ surfaces, (4) an extra-vascular PVS that runs along the exterior of large blood vessels, (5) a neural PVS that exists inside the brain and spinal cord and runs along the exterior of peripheral nerves, (6) an intra-organ PVS located inside various internal organs[20].

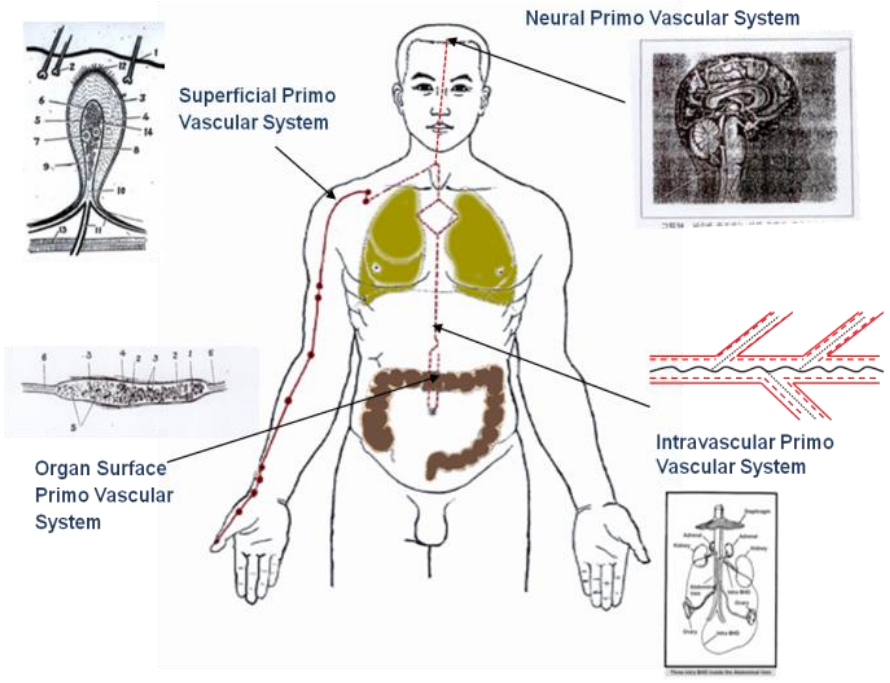

Fig.1.3. **A schematic drawing of PVS. Parts of PVS at various sites are shown.** (Illustrated by biomedical Physics Lab, SNU)

This extensive network of the PVS is composed of the three parts which are called primo nodes (PNs), and primo vessels (PVs) and the primo

fluids. The vessels are often sub-branched from each node [6, 8, 19] and the fluid contains primo microcells, which circulates in the PVS.

Figure 1.5 ((a) & (b)) shows the characteristics of PVS uniqueness compared to others. First, rod-shaped nuclei of endothelial cells (10-20 um) are linearly aligned along the PVs and it can clearly have revealed by DAPI (DNA-specific staining) [10, 11, 12]. Second, the PVS is composed of a bundle of several small ductules (10-50um) containing immune cells [13, 14, 15]. The ultrastructure of primo ductules in a primo vessel shared some common properties with blood and lymphatic vessels, but importantly, it possessed their own distinct structural features (figure 1.4) [19].

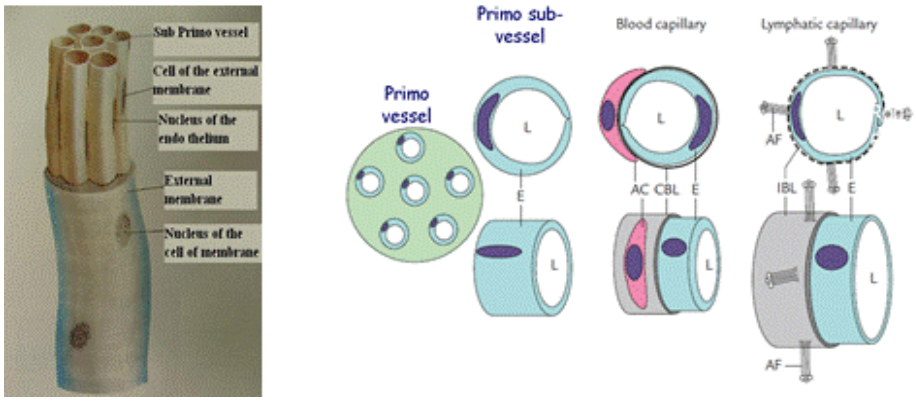

Fig.1.4. **Structural properties of primo vessel, blood and lymphatic capillary.** E: Endothelium, L: Lumen, CBL: Complete basal Lamina, IBL: Incomplete basal lamina. (*J Acupunct Meridian Stud* 2009; 2(2))

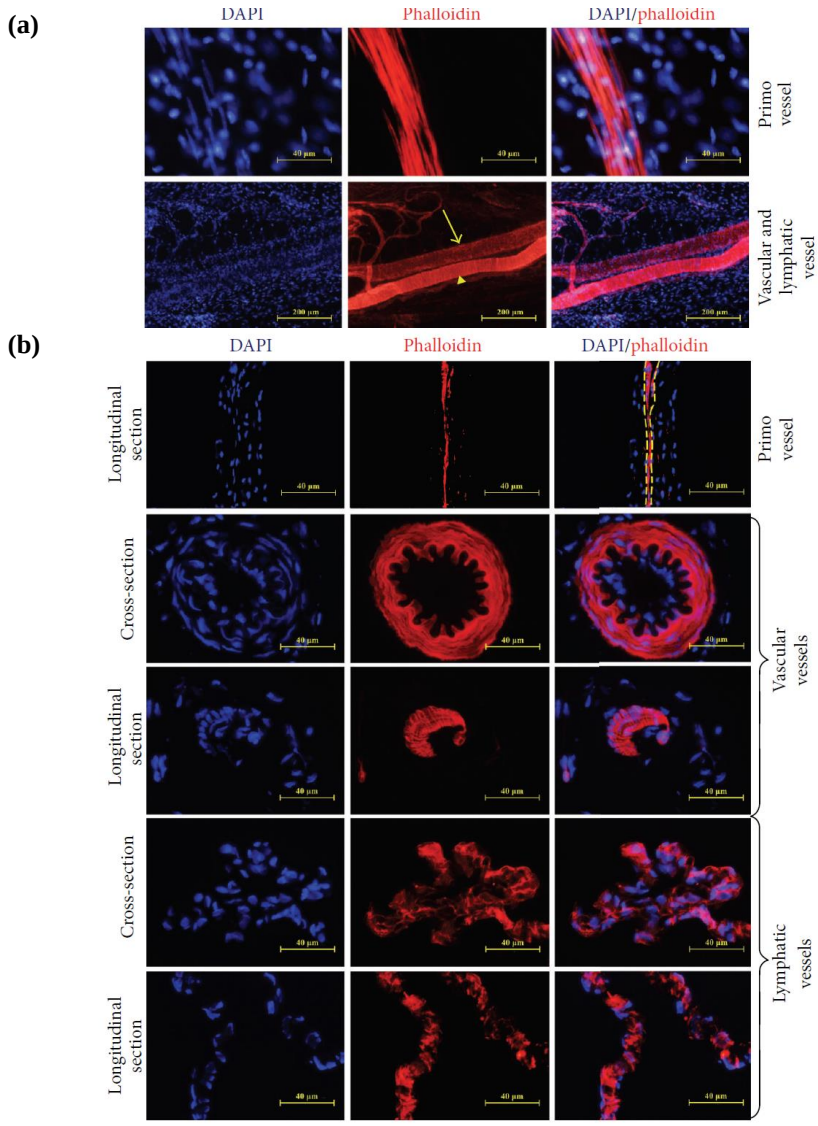

Fig.1.5. **<u>Comparison of the fluorescent staining in PV, Vascular and Lymphatic vessels.</u>**

The differences among primo vessels, vascular vessels, and lymphatic vessels. **(a)** Primo vessels consist of phalloidin positive cells with characteristic rod-shaped nuclei, linear arrangements paralleling with the vessels. Vascular smooth muscle cells were also sensitive to phalloidin but showed thoroughly different appearances (yellow arrowheads). In lymphatic vessel, the

endothelial cells formed the vessels in a network way (yellow arrows). **(b)** The differences among primo vessels, vascular vessels, and lymphatic vessels in cryo-sections. Phalloidin positive cells with rod-shaped nuclei; linear arrangements in longitudinal sections were primo vessels (yellow dashed area). Vascular vessels showed smooth muscular cells circulating the vessels and lymphatic vessels were formed in a network way. (*ECAM Vol 2013, Article ID 205951*)

Lastly, fig 1.6 shows that the PVS contains many kinds of immune cells especially high number of mast cells (MCs) and white blood cells (WBCs). With histological analysis, we confirmed these thread-like vessels are distinct in morphological structure and even some of them are located inside blood and lymph vessels (fig 1.7).

Resident Cells of Primo Node (PN)

Cells	mean (%)
mast cell	20.03 ± 4.32
Eosinophil	16.43 ± 5.58
neutrophil	5.00 ± 0.00
Histiocyte	53.57 ± 2.66
lymphocyte	1.00 ± 1.00
Immature cell	2.93 ± 0.12
Chromaffin cell	0.33 ± 0.29

Fig.1.6. **Composition of the resident immune related cells (including WBC) in PN.** (*Cytokine 60, 2012*)

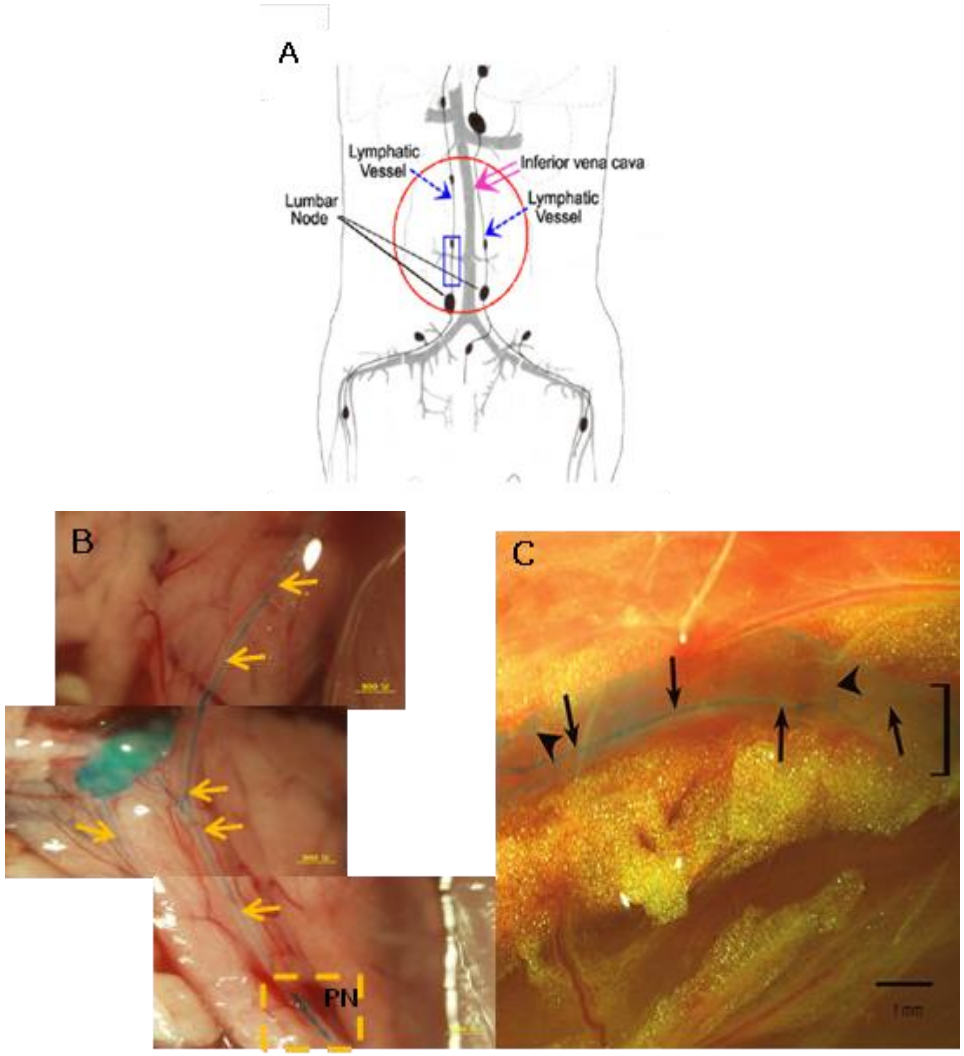

Fig.1.7. **<u>Morphological studies of PV isolated from lymphatic vessels</u>.** Stereomicroscopic images of alcian blue-stained PV. **(A)** Schematic diagrams of the lymphatic vessel and the lumbar node **(B)** A stereomicroscopic image of a stained PV within a lymphatic vessel and a PN. **(C)** An in-situ image of alcian blue-injected lymphatic vessel was captured. The hyaluronic-rich PV (arrows) is more prominently stained with alcian blue, while the surrounding lymphatic vessel (bracket) is weakly stained. Two luminal valves in the lymphatic vessel are also visible (arrowhead).

The main function of PVS is known as cell and tissue regeneration. However, the functional mechanism of this system is not yet fully understood. The gross anatomic morphology of this system could help compensate for this shortcoming [5]. PVS as an extension of acupuncture meridian system, these two will be treated as one system.

The therapeutic effects of acupuncture are being increasingly accepted worldwide [17, 18] and it is recognized as alternatives to western medicine, yet its mechanism of action is not scientifically confirmed fully. The anatomical reality of the meridian system has been controversial in various aspects. That is why it should be imperatively explained the mechanism of its effect in terms of modern scientific idea and terminologies. Still the many of people's question is whether the acupuncture meridian is a real physical being with channels containing flowing liquid. Then following question will be what is special about the meridians (AM) and acupuncture points (APs) and what makes so distinct them from other neighboring areas of the skin [19]. Thus, the anatomical structure of APs and AMs must investigate by researchers to answer above questions and understand mechanisms. Although it may be a very small step in a whole picture, the following experiments were conducted to approach the understanding of the pathology based on the PVS anatomical information. Even now the extensive reinvestigation with modern bio imaging techniques has been ongoing in this field.

References

1. Soh K.S, et al., “the primo vascular System: it’s role in Cancer and Regeneration”, Book from Springer Science and media; pp 3-5, DOI 10.1107/978-1-4614-0601-3_1
2. Soh K.S, et al., *“* The Primo Vascular System: Its Role in Cancer and Regeneration: proceedings from the first International Symposium on Primo Vascular System 2010 (*ISPS 2010*), with special topics on cancer and regeneration, September 17-18, 2010. Springer Science & Business Media. pp. 7–17.
3. Chan SH, et al., “What is being stimulated in acupuncture: evaluation of the existence of a specific substrate”, *Neurosci Biobehav. Rev* 1984; 8:25-33
4. Lee BC, et al., “Acupuncture muscle channel in the subcutaneous layer of rat skin”, *J Acupuncture Meridian Stud* 2008; 1(1): 13-19
5. Wick F, et al., “Morphological analysis of human acupuncture points through immunohistochemistry”, *American Journal of Physical Medicine & Rehabilitation*, January PP. 7-11, 2007
6. Lee BC, et al., “Electron microscopic study of novel threadlike structures on the surfaces of mammalian organs”, *Microsc Res Tech* 2007; 70: 34-43
7. HM Langevin, et al., “Evidence of connective tissue involvement in acupuncture”, F*ASEB J* 16: 872-874
8. Lee BC, et al., “DiI staining of fine branches of bonghan ducts on surface of rat abdominal organs”, *J Acupuncture Meridian Stud*, vol. 2, no. 4, pp. 301-305, 2009
9. Lee BC, et al., “Visualizing the network of Bonghan ducts in the omentum and peritoneum by using trypan blue”, *J Acupuncture Meridian Stud* 2: 66-70
10. Shin HS, et al., “Feulgen reaction study of novel threadlike structures (bonghan ducts) on the surfaces of mammalian organs”, *The Anatomical Record B: The New Anatomist*, vol. 284, no. 1, pp. 35-40, 2005

11. Yoo JS, et al., “In vivo visualization of Bonghan ducts inside blood vessels of mice by using an Alcian blue staining method”, *Indian Journal of Experimental Biology*, vol. 46, no. 5, pp. 336-339, 2008
12. Lee C, et al., “Alcian blue staining method to visualize Bonghan threads inside large caliber lymphatic vessels and X-ray microtomography to reveal their microchannels”, *Lymphatic Research and Biology*, vol. 4, no. 4, pp. 181-189, 2006
13. Lim CJ, et al., “Gross morphological features of the organ surface primo-vascular system revealed by hemacolor staining”, *Evidence-Based Complementary and Alternative Medicine*, vol. 2013, 12 pages, 2013.
14. Lee BC, et al., “Electron microscopic study of novel threadlike structures on the surfaces of mammalian organs”, *Microsc Res Tech* 2007 Jan: 70(1): 34-43
15. Kwon BC, et al., “Microscopic nodes and ducts inside lymphatics and on the surface of internal organs are rich in granulocytes and secretory granules”, *Cytokine*, vol. 60, no. 2, pp. 587-592, 2012
16. Ogay V, et al., “Comparison of the characteristic features of Bonghan ducts, blood and lymphatic System”, J *Acupunct Meridian Stud* 2: 107-117
17. Foster JMG, et al., “The mechanisms of acupuncture analgesia”, *Br J Hosp Med* 1987; 38:308−12
18. Son Y, et al., “Antipyretic efforts of acupuncture on the lipopolysaccharide-induced fever and expression of interleukin-6 and interleukin-1 beta mRNAs in the hypothalamus of rats”, *Neurosci Lett* 2002; 19:45−8
19. Libert C, “A nervous connection”, *Nature* 2003; 421:328−9
20. Soh KS, “Bonghan circulatory system as an extension of acupuncture meridians”, *J Acupunct Meridian Stud* 2009; 2(2):93-106
21. Kim BH, “Study on the reality of acupuncture meridians”, *J Jo Sun Med* 1962; 9: 5−13
22. Kim BH, “On the acupuncture meridian system”, *J Jo Sun Med* 1963; 90:

6−35

23. Kim BH, “The Kyungrak system”, *J Jo Sun Med* 1965; 108: 1−38
24. Kim BH, “Sanal theory”, *J Jo Sun Med* 1965; 108: 39−62
25. Baik KY, et al. “Acupuncture meridian and intravascular Bonghan duct”, *Key Eng Mater* 2005; 277-279: 125-9
26. Kang KA, "Historical Observations on the Half-Century Freeze in research between the Bonghan System and the Primo Vascular System", *Journal of Acupuncture and Meridian Studies.* **6** (6): 285–92
27. Kim BH, “Editor's Note", Great Discovery in Biology and Medicine: Substance of Kyungrak. Pyongyang: Foreign Languages Publishing House. p. 4 (1962)

Chapter 2

Observation of a Flowing Duct in the Abdominal Wall by Using Nanoparticles

(PLOS ONE | DOI: 10.1371/journal.pone.0150423 March 3, 2016)

Chapter 2

2.1 Introduction

The extensive network of the PVS was confirmed in various organs of mice, rats, rabbits, dogs, pigs, cows, and humans [2, 3]. Most of the previous experiments were done with vivi-staining of the PVS for its visualization using dyes such as trypan blue, alcian blue, chrome-hematoxylin and hema-color [4].

BH Kim's team reportedly used some blue dye to trace the acupuncture meridians and found the PVS network unexpectedly [1], but the method was not fully presented so that other independent groups can reproduce their results. Until the present time no one has been able to trace the acupuncture meridians by this type of method. The current work reports an interim progress in tracing the PVS which are near the conception vessel (CV) of a rat by injecting fluorescent nanoparticles (FNP) into a PN.

In acupuncture theory of meridians, the conception vessel runs along the linea alba where the acupoints CV 8 and 14 are at the umbilicus and the xiphoid, respectively, as indicated in fig 2.1(A). The abdominal wall fat band (AWFB) of a rat is located in the peritoneum side of the abdominal wall along the line corresponding to the CV [5]. There are prominent blood vessels in the AWFB running along the CV line. The caudal extension of the fascia becomes a ligament covering the bladder (fig 2.1(B)). The AWFB is indicated with an arrow, and the bulged fat tissue is covered by the peritoneum. A primo vessel (PV) came out of the AWFB (fig 2.1(C)) and joined the organ-surface PVS (OS-PVS).

Even though tracing of the complete path of a PV was not fully done the current work showed two important progresses: The fluid flowed in the PVS when injected into a PN, thereby proving that the PVS was a conduit

system [6]; The hard-to-detect PVS surrounded by connective tissues was, for the first time, detected with the aid of flowing rather than staining of a suitable agent.

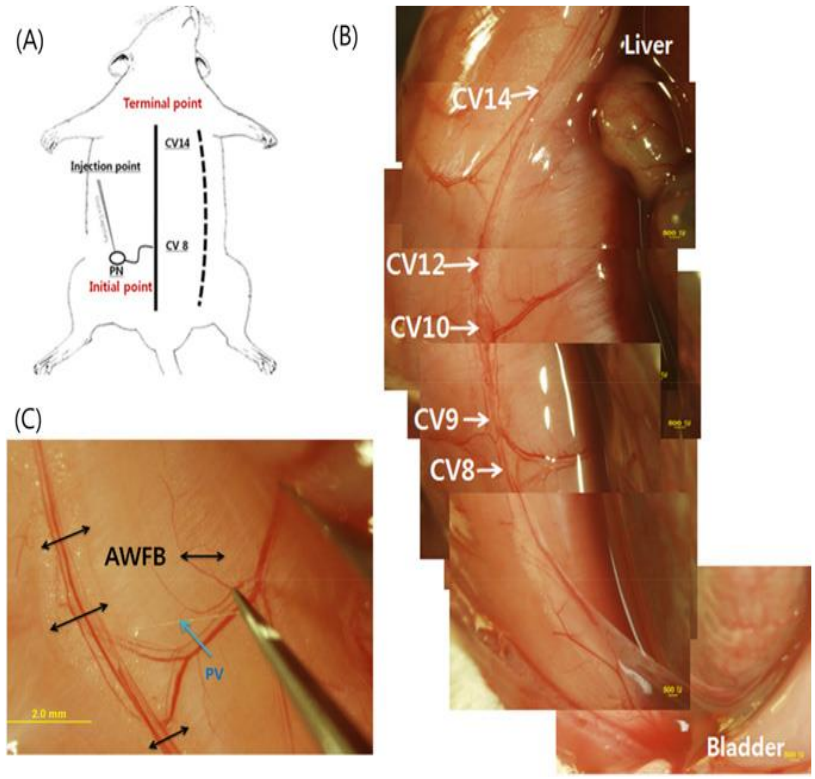

Fig.2.1. **The anatomical position of the novel flowing duct in the abdominal wall fat band.**

(A) Schematic illustration showing the location of linea alba and the conception vessel CV in the abdominal skin side. The broken line is the surgery cutting line of the abdominal wall. The line is in the right-hand side from the linea alba in order to avoid cutting the PVS in the AWFB. The FNPs that were injected to a PN entered the AWFB and appeared at the terminal point to be continued to the PVS on the liver surface. **(B)** The blood vessels in the AWFB inside the parietal peritoneum of the abdominal wall. The locations CV 8 to 14 are mere markings for positional references and not

real CV-acupoints. Note that the CV8 corresponds to the umbilicus and the parietal peritoneum continues down to the ligament wrapping the bladder. **(C)**: A PV (arrow) emerged from the AWFB (double arrows) was raised tautly with forceps.

In addition, the current work produced a significant understanding on why the PVS in skin such as the acupuncture meridians are difficult to observe in conventional histology. We demonstrated that the widely used hematoxylin and eosin (H&E) staining cannot distinguish the PVS from the wrapping connective tissue like the parietal peritoneum. Other staining with the Mason's trichrome or Toluidine blue did not work either. This explains why some histological efforts [7, 8] failed to detect the PVS at acupoints and meridians. The PVS is hard to recognize in the cross sections but is rather distinctively recognizable in the longitudinal sections with its characteristic endothelial nuclei distributions [9]. In the current work, we propose an effective method to find the PVS in skin: observation of mast cell distribution with toluidine blue staining which discriminate the PN from the lymph nodes because the latter has low density of primo nodes.

2.2 Material & Methods

2.2.1 Animal Preparation

The study was performed on sixty male Sprague-Dawley rats, 8–9 weeks old, medium weight 280 ± 10 g, which were obtained from DooYeol Biotech (Seoul, Korea). The rats were housed with a 12/12hr, light/dark schedule in a temperature- and humidity-controlled room, and had ad-libitum access to food and water. This study was carried out in strict accordance with the recommendations in the Guide for the Care and Use of Laboratory Animals of the National Institutes of Health.

The protocol was approved by the Institutional Animal Care and Use Committee (IACUC) of Woo Jung BSC, Inc. in conjunction with the Advanced Institute of Convergence Technology, Seoul National University. The rats were anesthetized by intramuscularly injecting a regimen consisting of 0.3 ml of zoletil and 0.1ml of rompun. All surgery was performed under deep anesthesia, all efforts were made to minimize suffering, and the rats were sacrificed by over-anesthetizing without any perfusion.

The entire processes of each experiment took two to three hours in deep anesthesia and no post-surgical analgesia was necessary. During the experiments, at least one of the researchers was on site and the conditions of the rats were continually observed. Since healthy rats were used there were no unexpected illness or dyeing occurred during the experiments. Our experimental protocol includes that at the end of the experiments and in the case of unexpected serious illness the rats should be euthanized by over-anesthesia.

An incision of the subcutaneous layer of the abdominal skin along the midline, but slightly off the linea alba, was performed with surgical scissors. We avoided cutting the linea alba in order to maintain the AWFB located at the midline of the ventral peritoneal wall because the target PNs are the AWFB (Fig 2.1B). All procedures of observations and operations were performed under a fluorescence tissue microscope (MVX10, Olympus, Japan). Once the desired PN was found we proceeded to the injection process. In the whole experiments, it was important to keep the PN humid by dripping phosphate buffer solution (PBS) or other suitable liquid onto the PN.

2.2.2 Injection and observation of fluorescent nanoparticles

Fluorescent nanoparticles (FNPs) were synthesized by modifying previously reported method [10]. Modified rhodamine B was incorporated in silica nanoparticles by co-condensation with tetraethyl orthosilicate in ethanol

with NH4OH and water. The average size of FNPs was 50 nm and FNPs had a photo-luminescence maximum at 547 nm with excitation at 450 nm. The surface of FNPs was functionalized with 2-[methoxy (polyethyleneoxy) propyl] trimethoxysilane (PEG-silane) in order to increase biocompatibility. The PEG modified FNP was dispersed in deionized water (10 mg of FNPs in 1 mL of deionized water).

The FNPs were injected into a PN by a glass capillary which was made sharp by pulling with the glass capillary puller (Narishige, PP830; Tokyo, Japan). In order to minimize the puncture of the PN the tip of the capillary was further sharpened with the Micro-Forge (Narishige, MF- 900; Tokyo, Japan). The injecting system was controlled by a home-made 3D manipulator. The glass capillary was connected to a 1ml hypodermic syringe which was supplied with the FNPs through the micro injector (KDS Scientific, KDS Legato 110, Daejeon, Korea). The fluid injection was done up to one hour with flow speed 500 nl /min.

The flow path of the FNPs was observed with a fluorescent tissue microscope (MVX 10, Olympus, Japan) in vivo in situ. In order to study the detailed histological nature of the path the AWFB was harvested and the magnified view of the flow path were recorded with the phase contrast microscope (BX-51, Olympus, Japan)

2.2.3 Histological Analysis

The isolated samples were fixed with neutral buffered formalin (NBF) at 23°C for 24 hr ± 2hr. The specimens were embedded in paraffin and cut to 5-µm-thick sections by using a microtome (Reichert Jung 820, Leica, Wetzlar, Germany). We performed hematoxylin and eosin (H&E), Masson's trichrome staining following conventional protocols, and picro-sirius red staining (PSR) staining. The protocol by Dolber was adopted for PSR staining [11]. The protocol for the toluidine blue was the same as the one used in [12].

The stained samples were examined under fluorescence microscope (BX-51, Olympus, Japan) with a CCD camera (Infinity 3–1 CCD Camera, Lumenera, USA).

2.3 Results

Fluorescent nanoparticles (FNP) were injected into a PN which was connected to a PV that came out of the AWFB around the point CV 6 near the bladder. Among the sixty rats we found suitable PNs which came out of the AWFB in thirteen rats and the successful injections were made three times. The reason was difficulty with injecting small amount of FNP in a long period over thirty minutes. In the successful cases, the FNP flowed in the PV along the CV line in the AWFB which were recorded at two hours after injection. The flow was observed from CV 6 to CV 14 at xiphoid where the PV came out of the AWFB and traced toward the surface of the liver, but further tracing was not possible.

The boxed region of fig 2.2 (A) was analyzed with a phase contrast microscope and the magnified view is shown in fig 2.2 (B). Without fluorescent imaging, the blood vessel and the fat tissue are easily seen but the primo vessel is difficult to notice. With fluorescence, the traces of nanoparticles are clearly manifested thus revealing the PV along the blood vessel (fig 2.2 (C)). This is the putative extra-vascular PV along a blood vessel. A PN was observed at a point which was not noticeable without fluorescence (fig 2.2 (D)), but its appearance was striking with the fluorescence of nanoparticles (fig 2.2 (E)). Its diameter was 250 μm, it was connected to PVs in both sides and a loop of PV was prominent.

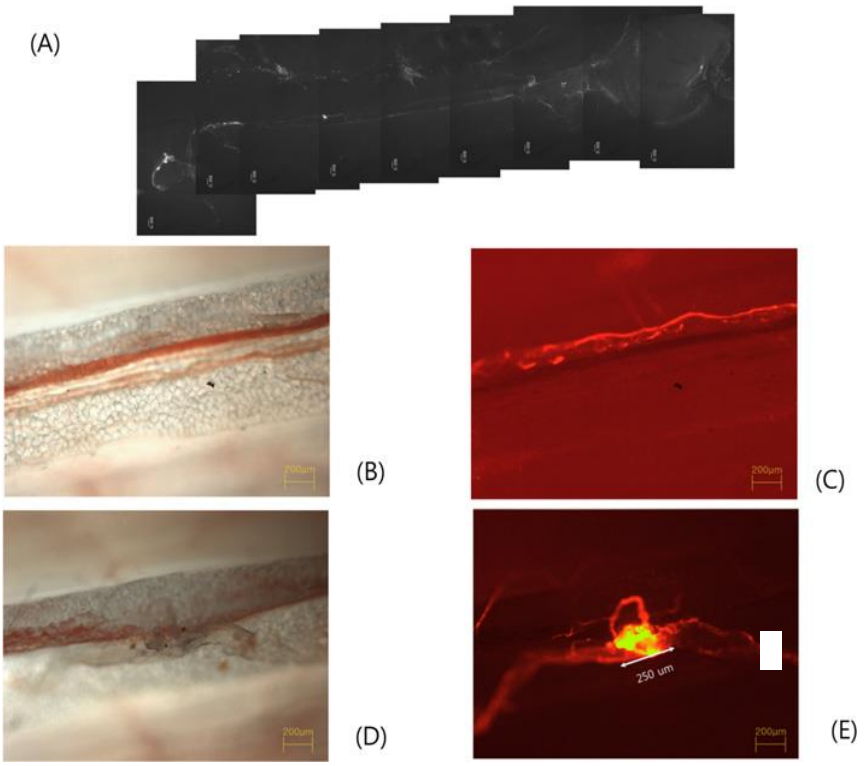

Fig.2.2. **Phase contrast microscope images of the PVS.**

(A) The fluorescent image of the FNPs that were injected at a PN located about the CV4 and flowed in a PVS buried in the adipose tissue of the AWFB. It flowed up to the CV 14 and reemerged to the abdominal cavity toward the liver surface. The flow line was barely visible under the stereo fluorescence microscope. **(B & C)** Phase contrast microscope images of the bright mode (B) and fluorescent mode (C) of the boxed region in (A). The PV (dashed arrow) running parallel to and above the blood vessel (two arrows) is hardly visible in (B) but clearly observable with fluorescence of FNPs in the panel (C). This primo vessel is the first observation of the so called extra vascular PVS. It runs closely along the blood vessel. The AWFB is clearly seen in (B) and its boundary is depicted with two curves in (C). The boundary of the abdominal wall fat band is indicated with two yellow curves (40x).

(D & E) The PN is not noticeable without the fluorescence in (D), but manifestly appears with fluorescent view in the panel (E). The size of the PN was 250 μm. The fluorescent nanoparticles were highly concentrated in the PN (40x).

Fig 2.3 explains why the PV was not observed in histology with H&E. The fluorescence image revealed the tiny spot of the PV just inside the peritoneum about 150 μm away from the blood vessel (fig 2.3 (C)). The region indicated in fig 2.3 (A) was analyzed with H&E staining and no noticeable structure was seen (fig 2.3 (B)) despite its presence was already proven. In another section, the PV was clearly denoted by the fluorescence of nanoparticles that flowed in it (fig 2.3 (D)). The Mason's trichrome discriminates muscle, deep fascia, peritoneum and fat tissue. But the peritoneum and PV could not be distinguished at all (fig 2.3 (E)). It is intriguing that the deep fascia and the parietal peritoneum are well distinguished, but the PV is undistinguishable from the surrounding parietal peritoneum.

The high density of mast cells in the PN [12] was confirmed here again. The presence of the PN was noticed by the fluorescent image of the nanoparticles that flowed in the PN (fig 2.4 (A)). In the PN that was inadvertently separated from the deep fascia a mast cell was observed after the toluidine blue staining (fig 2.4 (B)). An intact PN was obtained just inside the parietal peritoneum (fig 2.4 (C), 2.4 (D) and 2.4 (E)). Even though toluidine blue staining could not show any difference of the PV and the peritoneum it is useful for finding and identifying the PVS by the density of mast cells. In particular it is effective for discriminating lymph nodes and the PN as shown in fig 2.4 (C), 2.4 (D) and 2.4 (E).

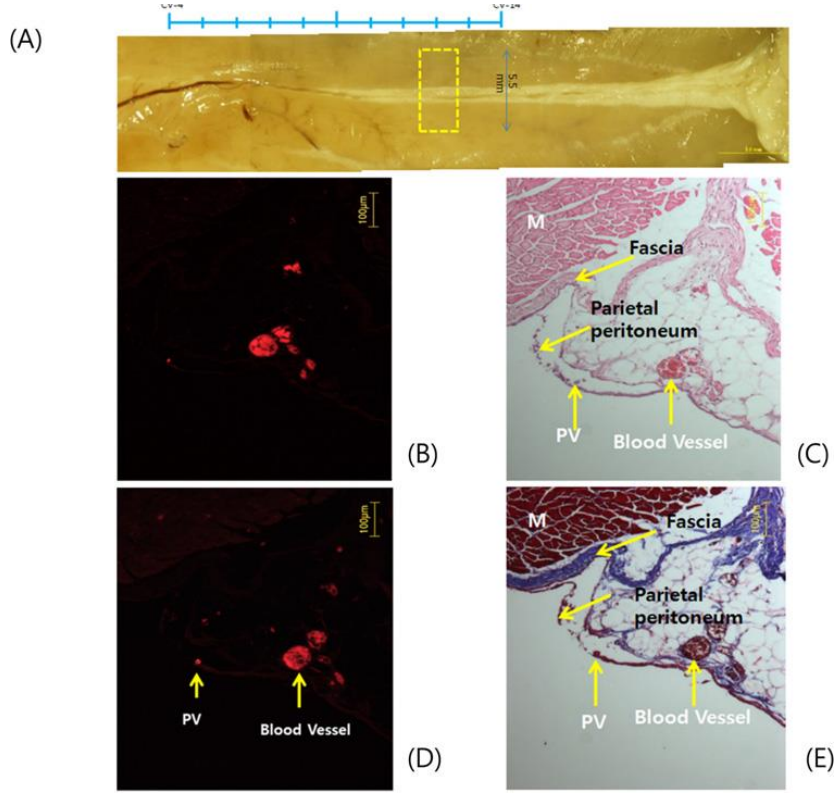

Fig.2.3. **Histological analysis of the PV, peritoneum and fascia.**

(A): The position of the tissue block for the cross section. (**B)**: The spot of fluorescence (arrow) due to FNPs is the position of the PV. Its size is 10 μm and 150 μm away to the left from the large blood vessel. (**C)**: The H&E staining barely revealed the spot of the PV (arrow) just inside the parietal peritoneum. This figure showed that the PV and the surrounding connective tissue of the parietal peritoneum are not distinguishable with H&E. The deep fascia and the parietal peritoneum are barely distinguishable. Muscle (M) is clearly distinguished by color. B &C are the same sections. (**D)**: Another section showed the fluorescence spot of the PV (arrow). (**E)**: The Mason's trichrome staining cannot distinguish the PV (arrow) and the parietal peritoneum. It can clearly distinguish the parietal peritoneum and the deep fascia. Muscle (M) is also well distinguished. D &E are the same sections.

2.4 Discussion

The flow of alcian blue in the PVS was tested in the OS-PVS and the flow speed was measured to be 0.3 mm/sec [6], which was a direct proof that fluid flows in the PVS. In other subsystems of the PVS it was not confirmed whether fluid flows in the PVS. The current study showed that nanoparticles flow in the PVS in the abdominal wall. More importantly, in this study, we found a novel PVS in the middle of the ventral abdominal wall as flowing duct connected to the OS-PVS. It is the first time to show that the PVS can be traced by injecting nanoparticles in a PN. Until the present time the only way to detect some subsystems of the PVS was to visualize them with some staining dyes. The classic work by Kim claimed that the full PVS network was discovered by injecting some blue dye into acupoints of rabbits, but no one could reproduce the results until the present time mainly because the injection methods and procedures were not described in detail [1]. The current work is a significant progress toward tracing of the full PVS network by injecting dyes into a PN.

The limitations of the current tracing experiment are its low repeatability due to the low probability of finding the PN at the abdominal wall. It was necessary to develop a surgery method to avoid cutting the PVS that was present in the AWFB. Therefore, the cutting line was on one side off the linear alba. Then it was difficult to evade the blood vessels. In addition, not all rats had the PVS at the expected position. However, through the training of the experimenter the statistics improved better and intact PNs were obtained as shown in fig 2.4. Another experimental skill was injecting very slowly the dye into a PN for a long time. Without this the tracing of the PVS for a long distance was not possible. Since the animal was breathing it was extremely difficult to puncture the PN with a micro capillary and keep it in the PN for a long period. Because of these technical difficulties the tracing was only done for a relatively short distance and we could not trace the PVS beyond the AWFB. In order to trace up to the skin and find the acupuncture

meridians technical improvements of the injection system are necessary.

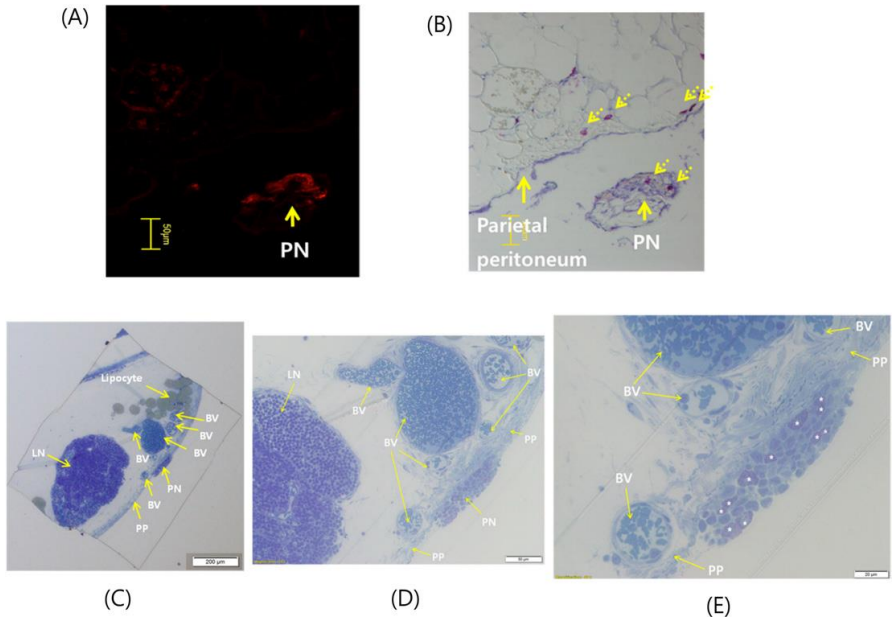

Fig.2.4. **Mast cells in the PN.**

(A) The fluorescence of FNPs indicates the location of a PN (arrow). (**B)** The toluidine blue staining cannot distinguish the parietal peritoneum and the PN. It showed the presence of mast cells (broken arrows) in the PN. The PN was torn off from the peritoneum during the sectioning process. (**C)** An intact PN stained with toluidine blue was obtained. The overview of an AWFB-section shows a PN which are well kept just inside the parietal peritoneum. A lymph node (LN), blood vessels (BV), adipose tissues and parietal peritoneum (PP) are also seen showing their relative locations. It is a rare and fortunate case that a lymph node and a PN located nearby was found as presented in this figure. **(D)** A magnified view shows that the cells in the lymph node and the PN look different. In fact, there were no mast cells in the lymph node and but many in the PN. (**E)** A further magnified

image depicts clearly the distribution of mast cells (*). The toluidine blue staining can be used for identifying the PN by revealing the abundance of mast cells even though it could not distinguish the collagens of the PN and surrounding connective tissues.

References

1. Kim BH, “The Kyungrak system”, *J Jo Sun Med*; 1965 108:1–38.
2. Soh K.S, et al., “The Primo Vascular System: Its Role in Cancer and Regeneration”, New York, Springer; 2011.
3. Soh K.S, “Hypothesis on the Treatment of Gliomas with Acupuncture at the Primo Node Corresponding to ST 36”, *Med Acupunct*. 2015; 27:144–150.
4. Lim C.J, et al., “Identification of primo-vascular system in abdominal subcutaneous tissue layer of rats”, *Evid-Based Compl Alter Med*. 2015; Article ID 751937.
5. Ogay V, et al., “Observation of Coiled Blood Plexus in Rat Skin with Diffusive Light Illumination.”, *J Acupunct Meridian Stud*. 2009; 2(1):56−65.
6. Sung B.K, et al., “Measurement of flow speed in the channels of novel threadlike structures on the surfaces of mammalian organs”, *Naturwissenschaften.* 2008; 95: 117–124
7. Kellner G Bau, et al., *Deutche Zeitschrift fur Akupunktur*; 1966 15:1–31.
8. Langevin HM, et al., “Relationship of acupuncture points and meridians to connective tissue planes”, *Anat Rec B, New Anatomist*.2002; 269:257–265.
9. Shin H.S, et al., “Feulgen reaction study of novel threadlike structures on the surface of rabbit livers”, *Anat Rec B, New Anatomist* 2005; 284:35–40.
10. Ha S.W, et al., “New method to prepare very stable and biocompatible fluorescent silica nanoparticles”, *Chem. Commun*.2009; 28:2881–2883.
11. Dolber P.C, et al., “Conventional and confocal fluorescence microscopy of collagen fibers in the heart”, *J Histochem Cytochem*. 1993; 41:465–469.
12. Gil H.J, et al., “Number Density of Mast Cells in the Primo Nodes of Rats”, *J Acupunct Meridian Stud* 2015; 8

13. Zhu Z, et al., “Morphometric observation on the mast cells under the acupuncture meridian lines”, *Zhen Ci Yan Jiu*. 1990; 15:157–158 [In Chinese].
14. Zhang D, et al., “Role of mast cells in acupuncture effect”: *A pilot study, Explore (NY)*. 2008; 4:170–177
15. Lee BC, et al., “Electron microscopic study of novel threadlike structures on the surfaces of mammalian organs”, *Microsc Res Tech*. 2007; 70:34–43.
16. Lee H.S, et al., “Evidence for the Primo Vascular System above the Epicardia of Rat Hearts”, *Evidence-Based Complementary and Alternative Medicine* 2013; 8. Article ID 510461.
17. Kwon B.S. et al., “Microscopic nodes and ducts inside lymphatics and on the surface of internal organs are rich in granulocytes and secretory granules”, *Cytokine* 2012; 60:587–592.
18. Lim C. J, et al., “Gross Morphological Features of the Organ Surface Primo-Vascular System Revealed by Hema color Staining”, *Evidence-Based Complementary and Alternative Medicine* 2013; 12. A.ID:350815

Chapter 3

Ultrastructure of a Mobile Threadlike Tissue Floating in a Lymph Vessel

(Evidence-Based Complementary and Alternative Medicine Volume 2016, A.ID 3064072)

Chapter 3

3.1 Introduction

The primo vessel (PV) afloat in the lymph flow as a mobile threadlike structure is hard to observe without a suitable staining. The most frequently used staining dye was alcian blue [8], and recently hollow gold nanoparticles were found to be more effective for visualizing purpose [9]. Although numerous articles on the observation of the lymphatic PVS were reported, there has not been a thorough study of the ultrastructure of the PV with transmission electron microscope (TEM).

A previous TEM study of a lymphatic PV showed only part of the PV cross section in comparison with a lymph vessel [10]. Therefore, the detailed histological characterization of the PV has not been given in comparison with the lymphocytes that surround the PV.

In this paper, we present the whole view of the cross section of the PV compactly surrounded by lymphocytes so that the characteristic histological difference of the PV from the lymphocytes can be seen despite their similar sizes. Consequently, the current work firmly establishes the existence of the PV by providing firm data showing its characteristic ultrastructure.

3.2 Materials & Methods

3.2.1 Animal Preparation

Rats (Sprague-Dawley, male, 7 weeks old (210～230 g) were obtained from DooYeol Biotech (Seoul, Republic of Korea) and housed in a temperature-controlled environment (23°C). All animals were exposed to a 12-hour light/dark cycle and were provided food and water *ad libitum*.

The procedures involving the animals and their care were in full compliance with current international laws and policies (*Guide for the Care and Use of Laboratory Animals*, National Academy Press, 1996) and were approved by the Institutional Ethics Committee of the Advanced Institute of Convergence Technology. The rats were anesthetized by intramuscular injection of a regimen consisting of 1.5 g/kg of urethane and 20 mg/kg of xylazine.

3.2.2 Visualization and Observation of the PVS

Rats were injected with alcian blue, and the 1.0% alcian blue (A5268, Sigma-Aldrich, St. Louis, MO, USA) solution in boiled phosphate-buffered saline (PBS, pH 7.4) was filtered by using a 0.22 μm membrane filter (Merck Millipore, Darmstadt, Germany). After the inguinal node had been exposed, the prepared 1.0 % alcian blue dye was injected into the node. The lymph duct from the inguinal node to the axillary node was exposed to observe the PV in it. After the rats were sacrificed by using an intracardiac injection of urethane (1 mL), the lymph duct, including the PV, was harvested for histological study.

To confirm the distribution of rod-shaped nuclei with 4,6-diamidino-2-phenylindole (DAPI), the specimen was stained with 300 nM DAPI (D1306, Invitrogen, MO, USA) solution for 20 minutes. The shape and distribution of nuclei were examined under a phase contrast microscope (Olympus, U-

LH100HG, Japan) and a confocal laser scanning microscope (CLSM; C1 plus, Nikon, Japan).

For the observations with TEM, the specimens of the PV within a lymph vessel were fixed in 4% paraformaldehyde and 2.5% glutaraldehyde in 0.1M phosphate buffer for overnight. After washing in 0.1M phosphate buffer, the specimens were post-fixed with 1% osmium tetroxide in the same buffer for 1 hr. The specimens were dehydrated with a series of the graded ethyl alcohol, and pure acetone. The specimen was embedded in Epon 812 and the polymerization was performed at 60°C for 3 days. The cross sections of the PV inside a lymph vessel were first studied with optical microscope images of the semi-thin sections (1 μm) of the specimen before taking ultrathin sections (60–70 nm) for TEM. These semi-thin section images helped us to find the appropriate location for TEM. Ultrathin sections (60–70 nm) were obtained by ultra-microtome (Leica Ultra cut UCT, Germany). Ultrathin sections collected on grids (200mesh) were examined in TEM (JEM 1010, Japan) operating at 60kV and images in the TEM were recorded by CCD camera (SC1000, Gatan, USA). Length on the electron micrograph was measured using GMS software (Gatan, USA).

3.3 Results

The lymph vessel we studied was the one starting from the inguinal node, running along the epigastric blood vessel in the skin and entering the axillary node (figure 3.1(a)). The PV in this lymph vessel was observed *in vivo in situ* as a mobile floating threadlike structure stained blue with alcian blue (figure 3.1(b)).

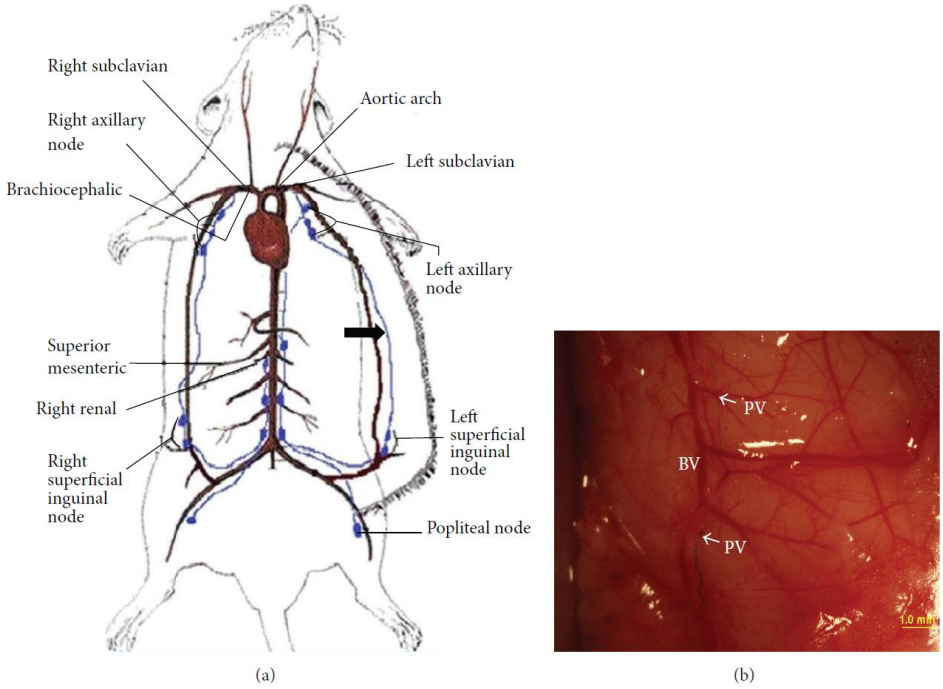

Figure. 3.1. **<u>Stereomicroscopic images of lymph ducts in which a PVS was stained with alcian blue</u>.**

(a) Illustration of the locations of the lymph nodes and ducts along the epigastric blood vessels (thick arrow) in skin. **(b)** The blue stained primo vessel (PV) in the lymph duct along the blood vessel (BV) is indicated with arrows. The lymph vessel is hardly visible in a stereomicroscopic image.

The lymph vessel with the PV inside was harvested as shown in figure 3.2(a). A piece of PV was extracted from the lymph vessel (figure 3.2(b)) and stained with DAPI for studying nuclei distribution in the PV. It was examined with a confocal microscope. As shown in the cross section view below the PV was not pure but rather thickly shrouded with lymphocytes; consequently, the nuclei seen in the surface of the apparent threadlike structure had round shapes. The optical sections of five μm thickness revealed the characteristic rod-shaped nuclei at the 15 μm depth from the surface of the extracted specimen whose thickness was 23 μm. It means the PV was located somewhat off-centered in the harvested specimen of the stained threadlike structure. The lengths of the rod-shaped nuclei were about 10 μm (figure 3. 2(c)).

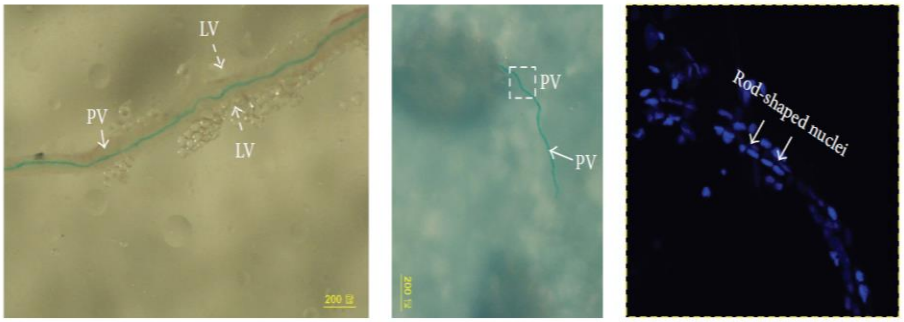

Fig.3.2. <u>Images of a harvested lymph duct in which a PV was stained with alcian blue.</u>

(a) A piece of the lymph vessel (LV) was harvested and image was taken with a phase contrast microscope. The PV is clearly seen due to the Alcian blue staining. **(b)** The stained PV was extracted from the lymph vessel with forceps. It was treated with DAPI to stain its nuclei. **(c)** The boxed region of the PV in (b) was examined with a confocal microscope. The rod-shaped nuclei of the endothelial cells of the PV were observed at the 15 μm depth from the surface of the stained threadlike structure whose thickness was 23 μm. The PV became thicker because it was covered with lymphocytes.

A piece of the harvested lymph vessel was embedded in OCT and its micro section was examined after de-freezing (figure 3.3 (a)). The Alcian blue stained threadlike structure containing the PV is clearly isolated from the lymph vessel which looked nearly void of lymphocytes. But another section we took for the TEM study was full of lymphocytes as shown in the toluidine blue stained semi-thin section (figure 3.3 (b)).

Among the deep dark blue stained lymphocytes in the lymph vessel laid the light blue stained PV. Thanks to the precise positioning of the PV in the semi-thin section we were able to identify the PV in the TEM images (figure 3.3(c)) which is a mosaic of several photographs to cover the whole lymph vessel. The PV is compactly surrounded by lymphocytes and is hard to recognize it unless its location is given by other means. The confounding factors are the small size of the PV and the thinness and softness of the surrounding membrane of the PV which makes the distinction of the PV from the adhered materials. Figure 3.3(d) shows the PV with its two endothelial nuclei and loosely scattered distribution of collagen fibers with many empty spaces.

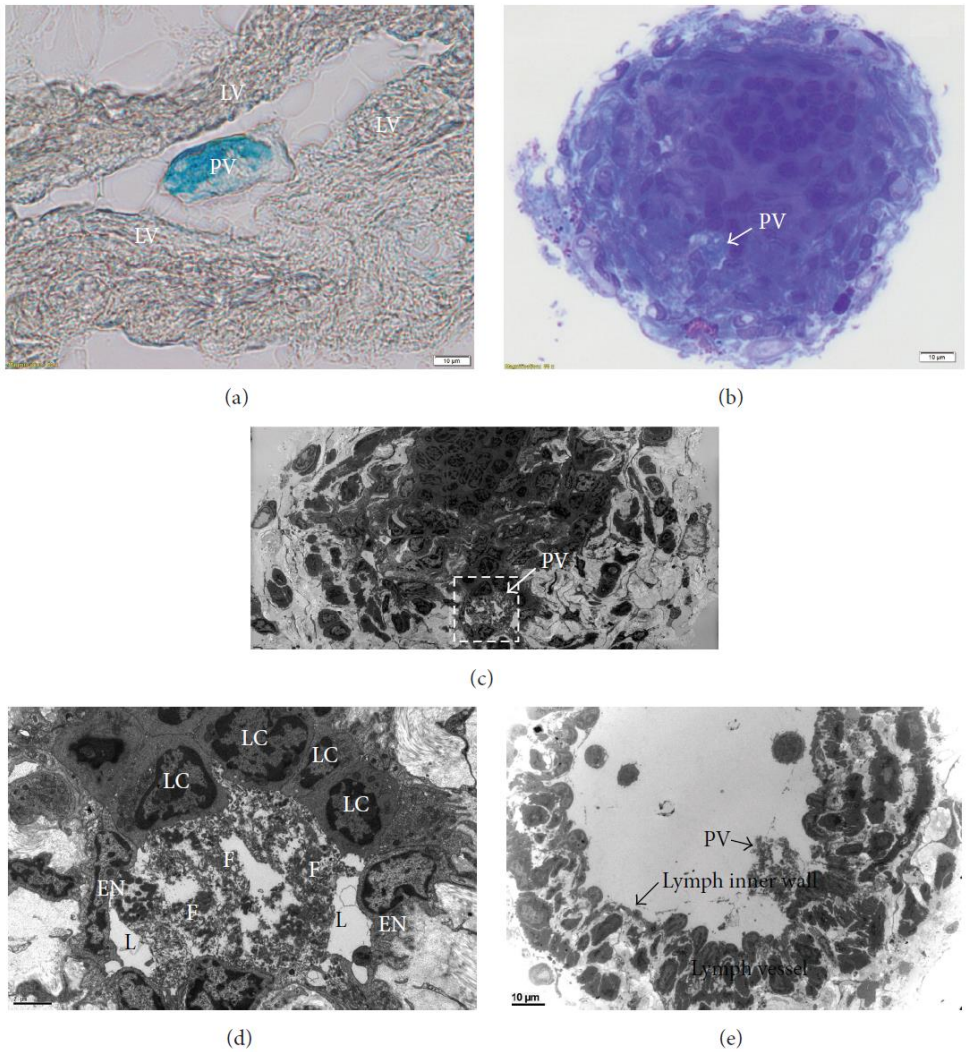

Fig. 3.3. **<u>Cross-sectional images of a PV in the harvested lymph duct.</u>**

(a) A cross section of the lymph duct (LV) with a blue stained PV in it. This specimen was frozen in OCT and the image was taken with a phase contrast microscope. This part of the lymph duct contained the PV without surrounding lymphocytes. **(b)** The semi-thin section of the toluidine blue stained lymph duct which were full of lymphocytes. The PV was located below from the center of the lymph duct and it was somewhat light blue colored because of the alcian blue. This image helped us to find the PV among the

lymphocytes. This semi-thin image is necessary for pointing the precise location of the PV, which is in turn helpful to apply TEM study. **(c)**The mosaic of the TEM images of the lymph duct which was full of lymphocytes. The location of the PV was identified with the aid of the above toluidine image. The PV showed the loose distribution of collagen fibers. **(d)** The boxed region of (c) is magnified to show the details of the PV. Two endothelial cell nuclei (EN) are seen along the lumens (L) which are different from the nuclei of the surrounding lymphocytes (LC). The collagen fibers (F) are extracellular materials filling most of the PV. **(e)** A lymph vessel in which a PV was found without surrounding lymphocytes. The PV has similar distribution of fibers and lumens as (d).

3.4 Discussion

The PV inside lymph vessel has been identified through several stages of examinations: The PV stained blue with Alcian blue *in vivo in situ* is to stay afloat unbroken and not crushed to pieces when the lymph vessel is pushed and moved by forceps. When the lymph vessel is harvested the PV should be strong enough to be extracted through a hole by pulling one end of the PV with forceps. Most critically, the PV after staining with DAPI should show the presence of the rod-shaped nuclei distributed in broken lines along the direction of the lymph vessel, which can be seen with a confocal microscope. Figures 3.1(b), 3.2(a), 3.2(b), and 3.2 (c) shows that the specimen we studied passed these identification criteria.

The main contribution of the present work was to show the ultrastructure of the PV in the lymph vessel with TEM images. Although the TEM images of the lymphatic PV were previously taken they were only small parts of the PV and lymph vessel [10]. This time we took the whole cross-sectional view of the containing lymph vessel and the PV. It showed the characteristics loose distribution of the collagen fiber with many empty spaces,

which was in good agreement with the previous work of the lymphatic PV [10] and the PV on the organ surfaces [11]. The thin surrounding membranes of the PV are another agreeing feature which is very thin as Kim described [3]. In addition, it revealed the endothelial nuclei and the lumens as shown in figures 3.3(c) and 3.3(d). This is the most important histological property that could be examined with TEM. This detailed ultrastructural characteristic can only be seen with TEM and is necessary to identify the PV in a complicated situation incurred by the accumulation of lymphocytes. Without the help of the semi-thin section stained with toluidine blue in figure 3.3(b) it would very difficult to locate the position of the PV.

The medical significance of the PVS is still to be investigated but data have already been accumulated showing its possible roles in innate immunity suggested by the abundant immune cells like mast cells in the PVS [6, 11]. There are also data showing the role as a source of very small stem cells [7], a path for metastasis [12], and a haven for cancer stem cells [13].

In conclusion, the study of the ultrastructural morphology of the lymphatic PV showed its detailed structure enough to identify the PV among the complicated situation when compactly surrounded with lymphocytes. This also explains how difficult it is to find the PV without careful and intentional search for it with TEM.

References

1. Park M, et al., “A modern clinical approach of the traditional Korean Saam acupuncture,” *Evidence-Based Complementary and Alternative Medicine*, vol. 2015, Article ID 703439
2. Lee MS, et al., “Randomized clinical trials of constitutional acupuncture: a systematic review,” *Evidence-Based Complementary and Alternative Medicine*, vol. 6, supplement 1, pp. 59–64, 2009.
3. Kim BH, “The Kyungrak system,” *Journal of Jo Sun Medicine*, vol. 108, pp. 1–38, 1965.
4. Soh KS, et al., “*The Primo Vascular System: Its Role in Cancer and Regeneration”*, Springer, New York, NY, USA, 2012.
5. Lim CJ, et al., “Identification of primo vascular system in abdominal subcutaneous tissue layer of rats”, *Evidence-based Complementary and Alternative Medicine*, vol. 2015, Article ID 7519376
6. Kwon BS, et al., “Microscopic nodes and ducts inside lymphatics and on the surface of internal organs are rich in granulocytes and secretory granules,” *Cytokine*, vol. 60, no. 2, pp. 587–592, 2012.
7. Lee SJ, et al., “Adult stem cells from the hyaluronic acid-rich node and duct system differentiate into neuronal cells and repair brain injury,” *Stem Cells and Development*, vol. 23, no. 23, pp. 2831–2840, 2014.
8. Lee C, et al., “Alcian blue staining method to visualize Bonghan threads inside large caliber lymphatic vessels and X-ray micro tomography to reveal their micro-channels,” *Lymphatic Research and Biology*, vol. 4, no. 4, pp. 181–189, 2006.
9. Carlson E, et al., “A novel technique for visualizing the intralymphatic primo vascular system by using hollow gold Nano spheres,” *Journal of Acupuncture and Meridian Studies*, vol. 8, no. 6, pp. 294–300, 2015.
10. Johng HM, et al., “Use of magnetic nanoparticles to visualize threadlike structures inside lymphatic vessels of rats,” *Evidence-Based*

Complementary and Alternative Medicine, vol. 4, no. 1, pp. 77–82, 2007.

11. Lee BC, et al., "Electron microscopic study of novel threadlike structures on the surfaces of mammalian organs," *Microscopy Research and Technique*, vol. 70, no. 1, pp. 34–43, 2007.
12. Yoo JS, et al., "Characterization of the primo-vascular system in the abdominal cavity of lung cancer mouse model and its differences from the lymphatic system," *PLoS ONE*, vol. 5, no. 4, Article ID e9940, 2010.
13. Islam M.A, et al., "Tumor-associated primo vascular system is derived from xenograft, not host," *Experimental and Molecular Pathology*, vol. 94, no. 1, pp. 84–90, 2013

Chapter 4

4.1 Superficial Primo Vascular System

4.2 Ogay Primo Node Study

4.3 Distribution of mast cells and locations, depths and sizes of the putative acupoints CV8 and KI16

(Evidence-Based Complementary and Alternative Medicine Volume 2017, A.ID 2953278,)

Chapter 4

4.1 Superficial Primo Node (S-PN)

4.1.1 Introduction

Superficial Primo node is an anatomical structure with a distinct boundary but has a very special histological structure. Its detailed morphological features were clearly described in Kim's article. The surface of the exposed S-PN is located in the reticular layer (dermis) of the skin in the AP position and linked loosely up with the connective tissue around them and its shape is an oval structure. The bottom-most part of the S-PN is connected with the bundle of blood vessels and PV. S-PN is seems to be more transparent than the surround tissues that could be the reason it can be hard to observe in bare eyes. Again, it has very unique external appearance (figure 4.1.1) [1].

In figure 4.1.1 shows that histological structure of the S-PN which can be subdivided into the subsections. Structurally speaking, each S-PN was a complex tissue structure consisting of an outer and inner layer. The S-PN comprises of the outer layer made up of smooth muscle and the inner layer made up of special cellular components and many capillary nets [1].

The outer layer made up of thick smooth muscle layer can be subdivided into outer circulating layer and inner longitudinal layer according to the direction the muscle fiber runs. At the tip of the superficial PN, the smooth muscle fiber radiating towards epidermis [1].

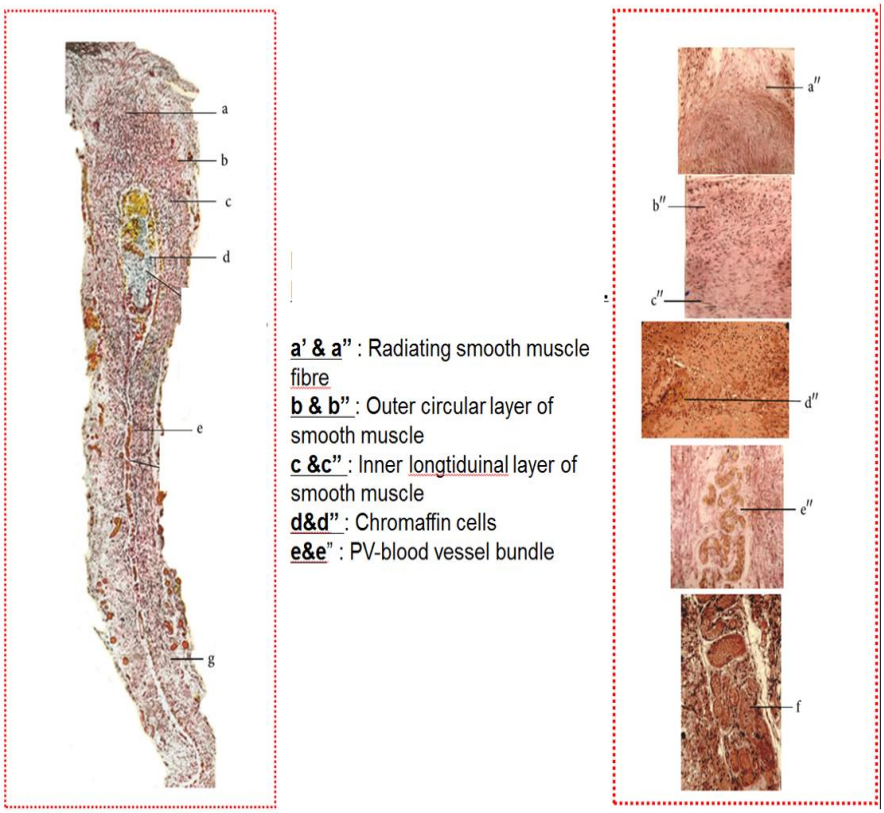

Fig.4.1.1. **Longitudinal section of superficial PN showing the histological structure**

(a) Profile of S-PN reported by Professor Kim **(b)** S-PN like structure of the young rabbit's umbilicus found in 1964 (c) Partial components of the umbilicus **(c)** PV: Primo vessel, : PV-like tubule; a, a', a" : radiation-like smooth muscle; b ,b', b": outer-circular layer smooth muscle; c , c', c": longitudinal layer smooth muscle; d, d', d", chromaffin cells; e , e', e": blood vessels, f : Fibrillenstruktur, g , g': elastic fibers, and h: skeleton muscle. (*from J Jo Sun Med, vol. 90, 1963 pages 6–35*).

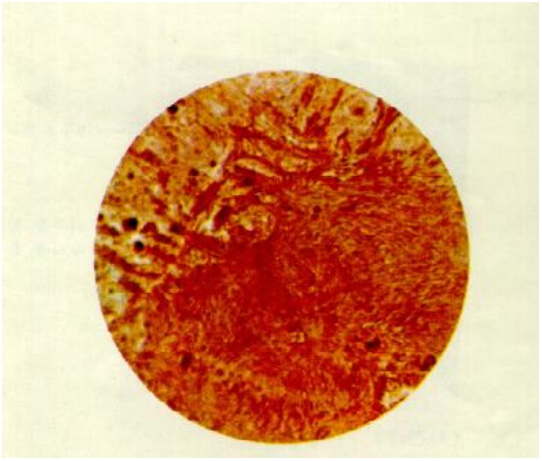

Fig.4.1.2. **Radiating smooth muscle fiber (cross-section) on the upper part of superficial PN**

(from book of great discovery in biology and medicine. 1962)

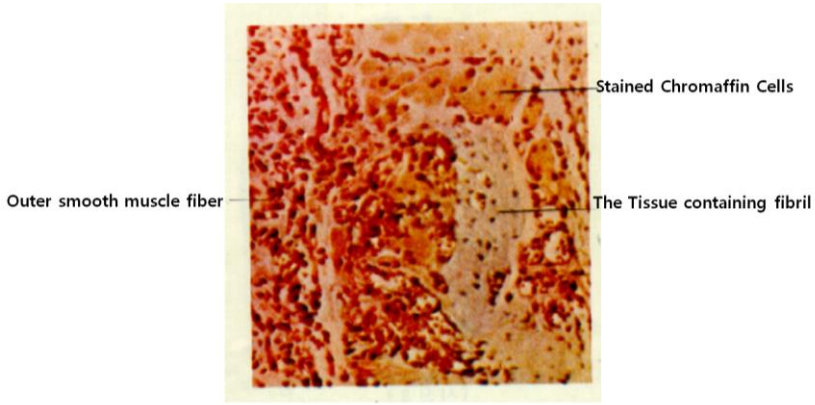

Fig.4.1.3. **Inner substance of superficial PN showing stained chromaffin cells and outer smooth muscle fiber.**

(from book of great discovery in biology and medicine.1962)

The inner substance of the S-PN comprises different kinds of cellular groups, fibers surrounding the cellular groups and well-developed capillary

networks. In all parts of the inner substance, chromaffin cells are distributed in rows around the blood vessel in small groups or scattered. The size of the chromaffin cell is known to be about 15-25 microns in diameter, its shape being round and oval. The inner substance has structures distinct from the connective tissues around it and from the chromaffin cells. These structures have fibrous structures that appear between them small granules that are sometimes basophilic and at other times acidophilic. The cytoplasm is stained yellowish brown by dichromate and filled with granules. In the central and lower parts of the inner substance, there is a follicular structure consisting of epithelial cells and smooth muscle cell types but we still have a question for the type of muscle cells. And there are dense capillary nets in the inner substance and the wall of follicular structure is made up of epithelial cells layers. This cell is about 12-20 um in diameter. [1]

In this experiment, our team focused to observe the morphological features of S-PN. First of all, we divide the observable parts in the section of cell (micro scale) and tissue (nano scale) types. The table 4.1.1 summarizes the targeted observable sections in detail.

	Optics (micro size scale work)	TEM (nano size scale work)
Mast Cell	Size/ Granules/ Distribution/ Location	Granules/ Nuclei
Chromaffin cell **	-Sympathetic nerve/ post ganglion	**Granules**: a lot of fine (low electron density) and coarse granules(high electron density) and many granular structures.
Smooth Muscle like cells **	-Follicular structure **Outer layer**: Thin (encircled by SM like cells), abundance of SM-like cells. **Inner layer**: Thick in longitudinal layer. -send out branches	**Nuclei** : -located near the inner substance (check chromatin) -thin membrane and their both ends usually have irregular contour; some membranes protrude and some others are indented. **Sacroplasm**: (cytoplasm of muscle cell) -the outer layer adjacent to the connective tissue surrounding the PN and reveals its inner structure due to extremely high electron density. -those bordering on the inner substance the structures of **myofibrils** and the **endoplamic reticulum** are recognized distinctly. -Fusion of irregular vacuolar structures at the end of the sarcoplasm. The structures thus formed contain either fine granular structures with lower electron density or irregular granular structures with higher electron density
Sinus **	-**Location**: Resorcinee Fuchsin or Verhoff staining method: The wall of sinus stains deeply- -Fulgen positive Check: Sinus's basophil의 유무 -**Shape**: Tubular ones formed of enlarged PV -**Branhching**	-Fibrous structures -The thickiness of the wall (**0.5-1um**) -Sponge like structures -intricately-branched **septal structures** and **small granular structures.** -Septum -**Sacroplasm**
Endothelial Nuclei **		Endothelial Nuclei: On the walls of many PV inside of the S-PN

Table 4.1.1. A summary table of substances can be found in S-PN

4.1.2 Materials and Methods:

4.1.2.1 Animals

Male Balb/c mouse aged postnatal of 3 days were obtained from Doo yeol laboratory Animal Company (Seoul, Korea). The animals were housed in a constant temperature-controlled environment (23°C) with 60% relative humidity. All animals were anesthetized with a mouse cocktail made with saline, zoletil and rompun.

4.1.2.2 Determination of Acupoints (APs)

The locations of the Conception Vessels (CV) meridian and acupoint CV12 were determined using an acupoint/ meridian map of animals. [2.3] The CV12 point can be easily identified and isolated on an animal body (figure 4.1.4 (B)). However, in the case of young aged mouse (up to post-natal 14 days), its CV meridian is still very weak and not tightly fixed in the abdominal skin yet.

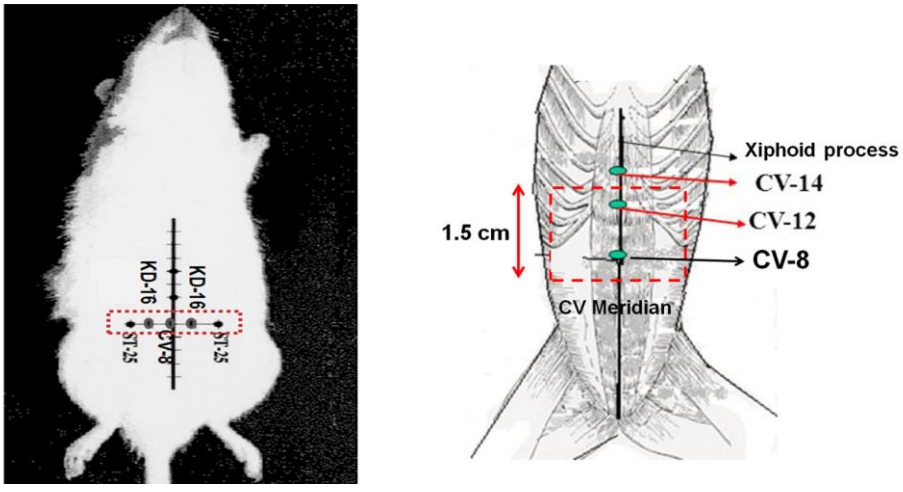

(A) (B)

Fig.4.1.4. An acupoint /meridian map of a mouse

(A) A picture showing the putative superficial-PN (CV8, KD 16 & ST 25) in ventral skin of a rat model. (B) Schematic illustration of the location of the CV meridian and acupoint in CV8, CV12 & CV14 in mouse. CV 8 and CV 12 are located on the ventral midline of the abdomen. CV 12 is the half distance between xiphoid process and CV-8.

4.1.2.3 Transmission Electron Microscopy (TEM)

Fixation

For transmission electron microscopy (TEM), tissues were fixed with 2.5% glutaraldehyde in 100 mM phosphate buffer at pH 7.0 solution at 4°C for less than 4 hours then followed by post-fixation in 1% OsO_4 in 0.2M sodium-cacodylate for 1hr, dehydrated with ethanol and propylene oxide, and embedded in Epon 812. Fixation is the first and most important step in TEM, if the mistakes made at this stage, the whole preparation becomes useless. Dehydration through a series of ethanol or acetones and propylene oxide are required [4].

Tissue Sample Preparation:

To examine the nano-scale morphological features of APs (CV8, KD 16 and ST 25), we trimmed the sample block with the changing the range from 5 um to 100 um until it reaches the targeted area (figure 4.1.5). Close to the area of APs (CV8), then the block cuts in 1um semi-thin sections for viewing with toluidine blue staining. From these sectioned stained specimens, we check for the features of mast cells (MCs), blood plexus and connective tissues in designated area. After detecting the interest area in specimen, for detailed observation, cutting the block to make ultrathin sections (50-80 nm) and collected on large-scale copper grids, contrasted using 2% uranyl acetate and Reynold's lead citrate, and examined under a transmission electron microscope.

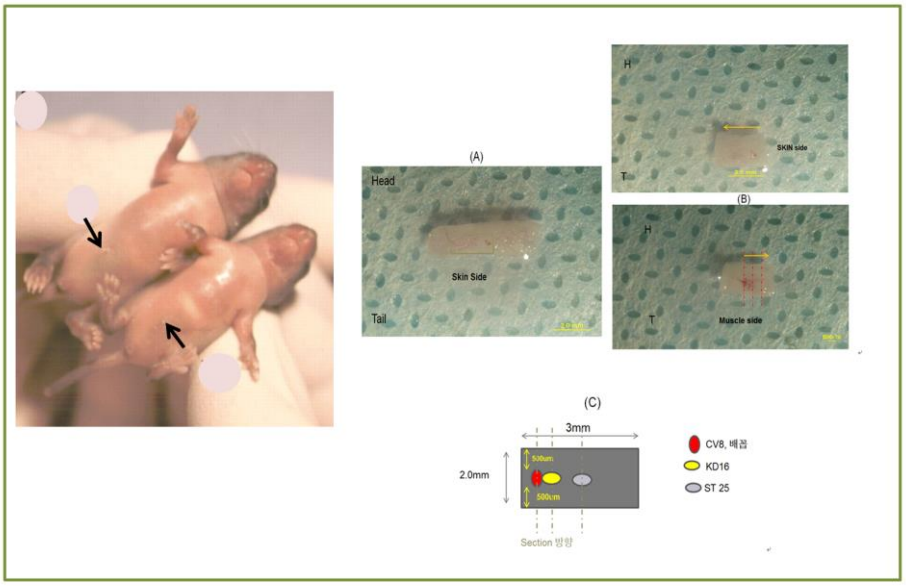

Fig.4.1 5. **Descriptive pictures of the sample block preparation**

It is very obvious to recognize the umbilicus (CV8) in young mice as indicated in picture with arrow. **(A & B)** A trimmed block is ready for the section in size of 3 mm x 2 mm. **(C)** A schematic illustration of the APs position in the trimmed block (A).

4.1.3 Results

4.1.3.1 Superficial PN and PN like structures.

Through the routine procedure of sample preparation, sectioning, toluidine blue staining, and light microscope, we observe the similar structure to superficial PN in the location of CV8 acupoint which is the location of umbilicus of young mice as Dr. Kim's described.

For clear comparison of the results, we have selected two different age groups of mice which were the post-natal 3 days and 8 weeks old. The reason of giving this variation was to show the distinct morphological difference in CV8 location. In this paper, we will present the result of the post-natal 3 days model.

The paper published in 2013 from the other group, they concluded that superficial PN like objects were only observed from the umbilici of the young rabbits even though they conducted a wide variety of experiments in different kinds of groups of animals including human corpses [9].

Our findings in here provided an opportunity to correct the conclusion provided from the other group. However, in our case, eight weeks old mice did not reveal the clear boundaries of superficial PN at all compare to the three days post-natal model. Thus, with careful prediction that the CV lines which were not firmly attached to the abdominal skin in young animal somewhat it might have the influence to it.

Under the light microscope and TEM analysis, chromaffin cells could not detect this time. However, an oval shaped structure was identified in the continuous sectioned images smooth-muscle like cells were observable in the outer layer. As you can see from the fig. 4.1.7 (B) &(C), the middle part of oval shaped APs was divided into two layers and three sections. Different compartments were seen in each layer (fig 4.1.7 (A) & (B)). In fig 4.1.7 (C) box 1 showed the radiating muscle fibers towards the epidermis but in this image, it was hard to distinguish the types of muscle. In box 2 clearly shows the outer boundary of S-PN and lastly the deep S-PN like object showed the packed of cells such as immune cell (macrophage and mast cells), plasma cell and blood vessels in the most inner layer of the S-PN.

(A)

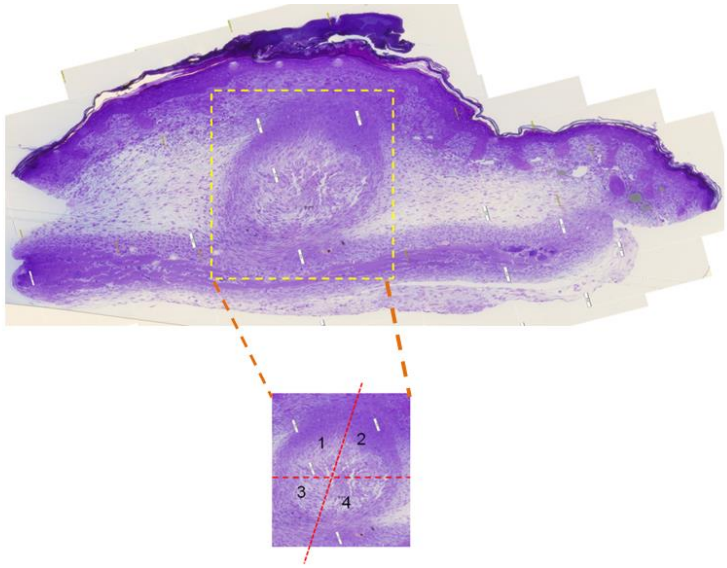

(B)

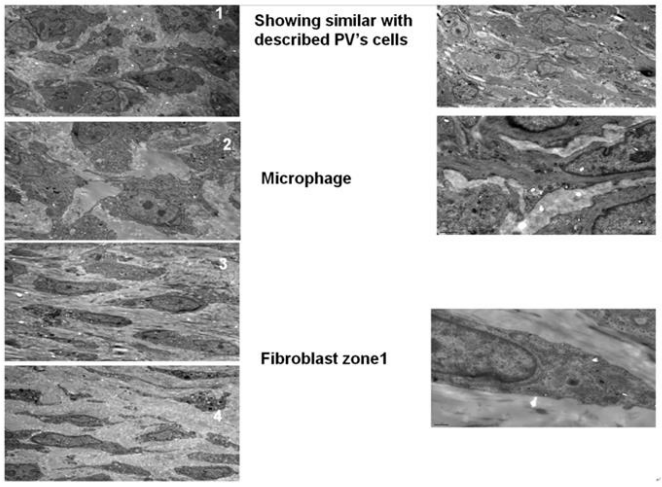

Fig.4.1.6 **Putative S-PN found on CV8.**

(A) Superficial PN like structures founded in CV8 was shown in post-natal 3 days model. Boxed region is corresponded to the area of CV8. **(B)** In the enlarged view of (A) box, the numbers showing in the boxed picture matches with the components we had observed in TEM image. (1-4) TEM images show the consisting components in putative S-PN.

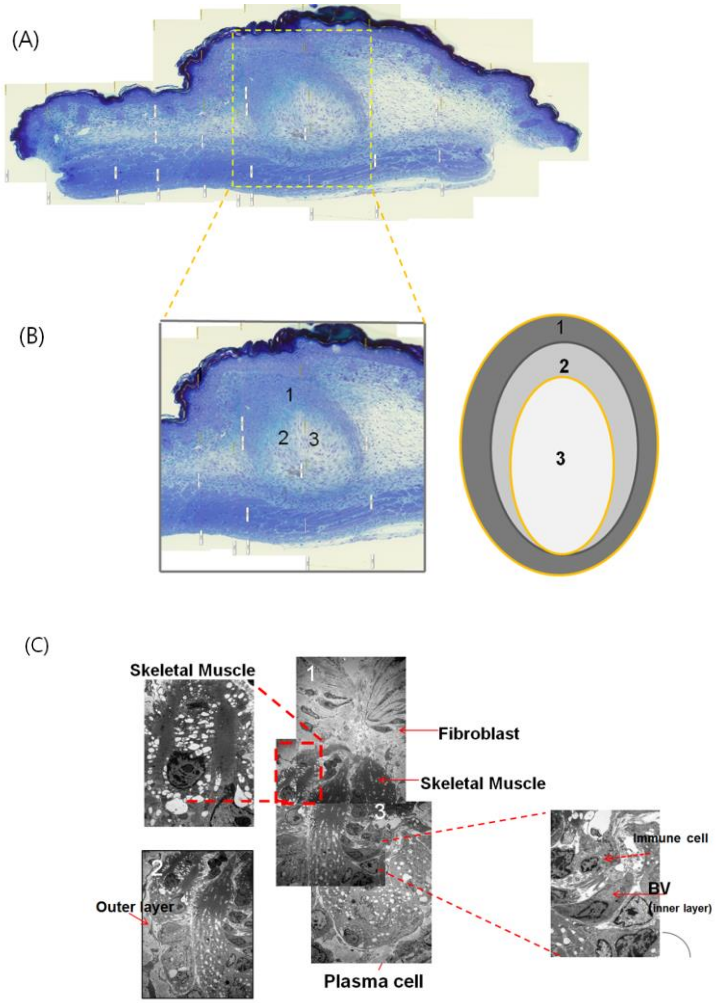

Fig.4.1.7 **Analysis of cells founded in the putative S-PN on CV8 location.**

(A) A semithin section stained with toluidine blue shows the S-PN at CV 8 region. **(B)** Magnified view of rectangular box (A) and illustration of structure in layers that correspond to boxed image of (B). **(C)** TEM analysis image of In box region (B) shows the radiating fibers towards the epidermis (1), the outer layer of S-PN (2) and the most inner layer of S-PN were packed with immune cell, plasma cell and blood vessels as Kim described (3).

4.1.4 Discussion

Just as those mentioned in the present paper, we tried various methods to observe and reproduce the superficial PN or PN-like structures in mice. But only in the young mice's umbilicus (CV8) showed the similar morphological evidence as the Dr. Kim claimed. However, there are still questions remained to be answered such as why only young animal groups can be shown this structure, which method could be suitable to differentiate the substances in different inner layer effectively and so on.

This report has shown evidence that the internal structure of the putative S-PN from the young mice model, however, we can't confirm this finding firmly due to lack of information. Thus, further investigation is required for the histological and morphological ultrastructure analysis that those are related to physiological factors. These points should be dealt in future studies using more cutting-edge technology.

Even despite the fact that the many evidences were provided by researchers which can explain the existence of meridian phenomena in the body, still there are only limited explanations by using current biological theories can be possible [10-14]. The only way to answer to this phenomenon is to solve the mystery of the primo vascular system

References

1. Kim BH., "*Great discovery in biology and medicine*", Foreign Language publishing House, Pyongyang, August 1962 pp 3-7
2. Deadman P, et al., "A manual of acupuncture." East Sussex: *Journal of Chinese Medicine Publications*, 1998:253.
3. Schoen AM., *Veterinary Acupuncture: ancient art to modern medicine*, 2nd ed. St. Louis: Mosby Inc, 2001:147.
4. Lee BC, "Novel Threadlike Structures on the Surfaces of Mammalian Abdominal Organs are Loose Bundles of Fibrous Stroma with Microchannels Embedded with Fibroblasts and Inflammatory Cells", *Connective Tissue Research*, 2013;54(2): 94-100
5. Li A, et al., "Human acupuncture points mapped in rats are associated with excitable muscle/skin-nerve Complexes with enriched nerve endings. *Brain Res* 2004; 1012: 154−9.
6. Langevin HM, et al., "Relationship of acupuncture points and meridians to connective tissue planes. *Anat Rec B New Anatomist* 2002; 269: 257−65.
7. Langevin HM, et al., "Mechanical signaling through connective tissue: a mechanism for the therapeutic effect of acupuncture. *FASEB J* 2001; 15: 2275−82.
8. Langevin HM, et al., "Evidence of connective tissue involvement in acupuncture. *FASEB J* 2002; 16: 872−4.
9. Liu JL, et al, "Historical Review about Research on "Bonghan System in China", *Evidence-Based Complementary and Alternative Medicine* volume 2013 (2013), Article ID 636081, 7 pages.
10. Lee BC. et al, "Bonghan ducts on the surface of rat internal organs." *J.Intl.Soc. Life Info*. Sci. 22: 455-459
11. Jung JH, et al., "Fine structure of extracellular fibers in primo-nodes and vessels." *Connective Tissue Res*. 52: 487-495

12. Yoo JS, et al., “Cribriform structure with channels in the acupuncture meridian-like system on the organ surfaces of rabbits.” *Acupunct. Electro-Therap. Res*. 32:130-132
13. Ogay V, et al., “Comparison of the characteristic features of Bonghan ducts, blood and lymphatic capillaries.” *J. Acupunct. Meridian Stud*. 2:107-117
14. Kim JD, et al., “Catecholamine-Producing Novel Endocrine organ: Bonghan system.” *MEDICAL ACUPUNCTURE*, Volume 20, Number 2, 2008
15. Freeman, et al. “Catecholamines in murine bone marrow derived mast cells.” *J Neuroimmunol* 2001; 119: 231−8.
16. Verhofstad AA, et al., “Immunohistochemical and biochemical study on the development of the noradrenaline- and adrenaline-storing cells of the adrenal medulla of the rat. *Cell Tissue Res* 1985; 242: 233−43.
17. Kierszenbaum AL., “Histology and cell biology: an introduction to pathology.” St. Louis: Mosby Inc., 2002:516.
18. Jones JP, et al., “Ultrasonic visualization and stimulation of classical oriental acupuncture points. *Med Acupunct* 2004; 15:24−6.

4.2 Ogay Primo Node Study

Acupuncture point (AP)'s one of key characteristic features is blood-nerves plexuses. This neurovascular bundle is a complicated plexus of nerves and blood vessels. Fig 4.2.1 (A) & (B) show clearly anatomical position of plexuses. Extending to the study of superficial primo node, we observed a series of neurovascular bundle along the besides of left and right stomach meridian lines in the abdominal skin of mice. It may not be detected only in mice but this time we would like to present the case of post-natal three days and eight weeks old mice model. The name of Okay node was named after the first detector of this structure on 2009.

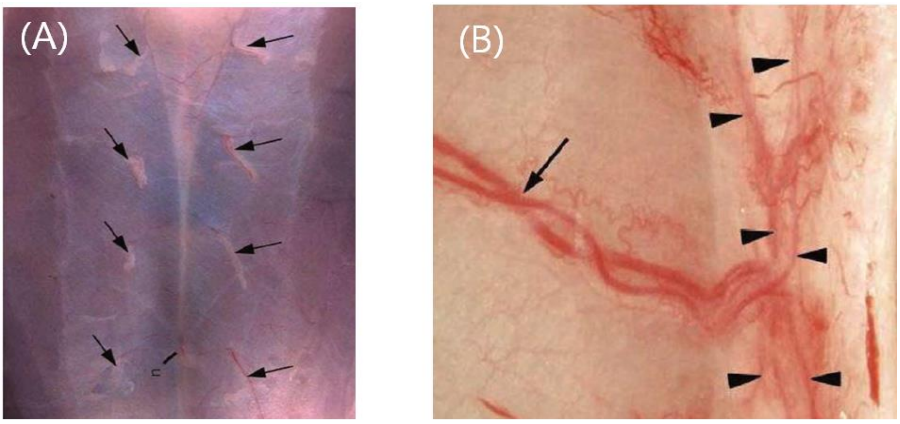

Fig.4.2.1. <u>Morphology and anatomical distribution of the neurovascular bundles (NBs)</u>

(A) View of the anatomical distribution of the NBs (arrow) along K-meridians on the abdominal skin area. **(B)** NB (arrow) forms several branches of blood vessels (arrowhead) in the subcutaneous layer. (*J Acupunct Meridian Stud 2009:2(1)*)

This complicated structure was firstly identified in previous study on 2009, but this topic of research was not continued and re-discovered this structure again during the finding skin primo nodes. The difference between these two experiments was testing animals.

Dr. Kim claimed to find specific corpuscular structures at the acupoints [2], but due to the difficulty of observing the structures, his theory was not confirmed yet. However, many followed studies were described APs as neuromuscular bundles [3, 4], neuromuscular attachments [5-8], and various types of sensory nerve endings. [9-11] Therefore, in this present work we aimed to investigate the mice abdominal skin to search for the neurovascular bundles as key distinguishing features of acupoints. We had been searching this complex structure in the corresponding area of kidney (KD) and stomach (ST) meridian lines and found set of blood vessel-nerve bundles located close to the ST meridian lines. Many studies aimed to find an analysis method to differentiate APs from surrounding tissues [1]. We have been trying to develop a method which will be applicable for identification of the APs in skin area but the results such as location and size were came up differently compared to the previous study, it was not succeeded this time.

As we discovered, the plexus we usually found in the skin has a distinguishable shape in the location below the hypodermis and just above the superficial fascia. It was easily detected by toluidine blue staining technique and checked that its size difference thorough continuous sectioned slides.

For finding its exact location, we measured the distance of KD-meridian and ST-meridian lines from conception vessel where the umbilicus (CV8, AP) located using meridian map of animals (fig 4.2.2 (A) & (B)) and finger cun unit method. To calculate the cun for the mice, we determined the anatomical location for CV8 and CV16 (xiphoid-sternal process) then we determined CV 12 on the linea alba (ventral midline) of the abdomen which was the midpoint between CV8 and CV16. Having the distance founded between CV8 & CV 12 divided by 4 then this value is equal to 1 cun [1]. Using this value, we calculated the location of APs on KD & ST meridian lines. Figures 4.2.3 (A) ~ (D) clearly show the calculation method and as you can see that there are differences between the mice models depending on the age.

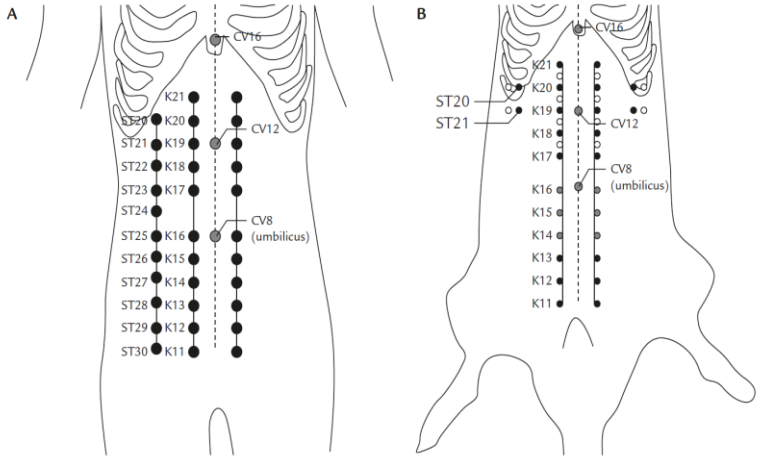

Fig.4.2.2. **<u>Relationship of the neurovascular bundles (NBs) and the acupuncture points (APs) on KD and ST meridian in rodent.</u>**

(A) Schematic illustration showing the locations of APs in a human. **(B)** Distribution of the NBs and mapped APs on K- and ST-meridians in the rodent. (*J Acupunct Meridian Stud 2009:2(1)*)

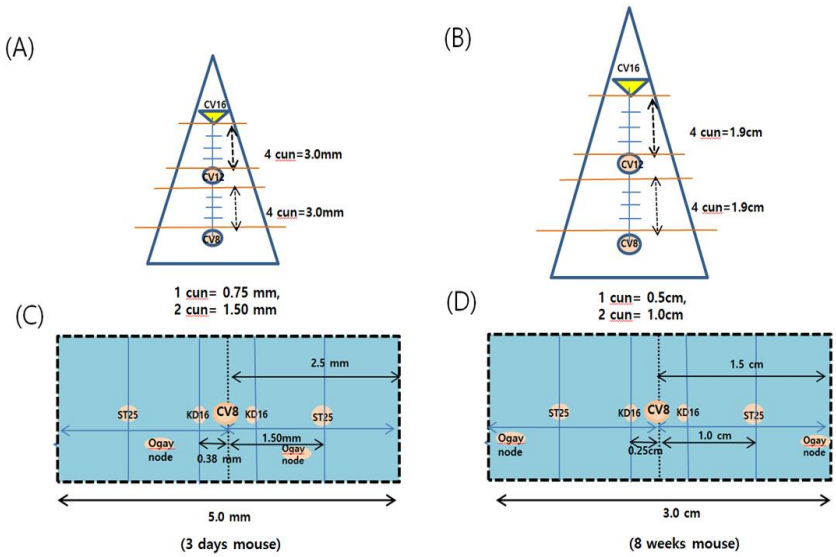

Fig. 4.2.3. **<u>Schematic diagram showing the distance of putative APs and ogay node for post-natal 3 days and 8 weeks mouse model.</u>**

(A) & **(C)** show the method of calculation and the location of APs and ogay node of 3 days old mice **(B)** & **(D)** show the

method of calculation and the location of APs and ogay primo node of 8 weeks old mice

After the anesthesia, we marked the corresponding location of APs on KD / ST meridian lines on the abdominal skin and carefully made a cut whole ventral skin section first and then mad a cut again to a small piece but including up to ST meridians lines bilaterally for analysis purpose. In this removed abdominal skin sections was stained with toluidine blue staining dye. It was useful for visualization under a stereomicroscopy.

One cun for the three days old of post-natal mouse (figure 4.2.3 (A) & (C)) was approximately 0.75 mm. This value was used to determine the locations of APs and meridians on the abdominal skin of mouse [1]. For example, KD and ST meridian line were located 0.38 mm (0.5 cun) and 1.5 mm (2.0 cun) lateral to the midline. And for the eight weeks mouse model (figure 4.2.3 (B) & (D)), 1.0 cun was approximately 5.0 mm. This value became reference value to determine the locations of APs and meridians. The KD and ST meridian line were located 2.5 mm (0.5 cun) and 10 mm (2.0 cun) lateral to the midline.

Then we examined whether marked APs locations correspond to anatomical locations of the neurovascular bundles. However, data from two groups (3 days & 8 weeks model) show different results. In figure 4.2.5 (C) revealed that ogay nodes (neurovascular bundles) located close to ST 25 meridian however 4.2.5 (D) was showing that ogay nodes located far behind the stomach meridian lines. The distance was between the range of 870~960 um for the 3 days and 1550 ~ 1850 um for 8 weeks model respectively. These results came different from our hypothesis and previous study. It is our thought that these variations could be caused by the growth cycle of mice.

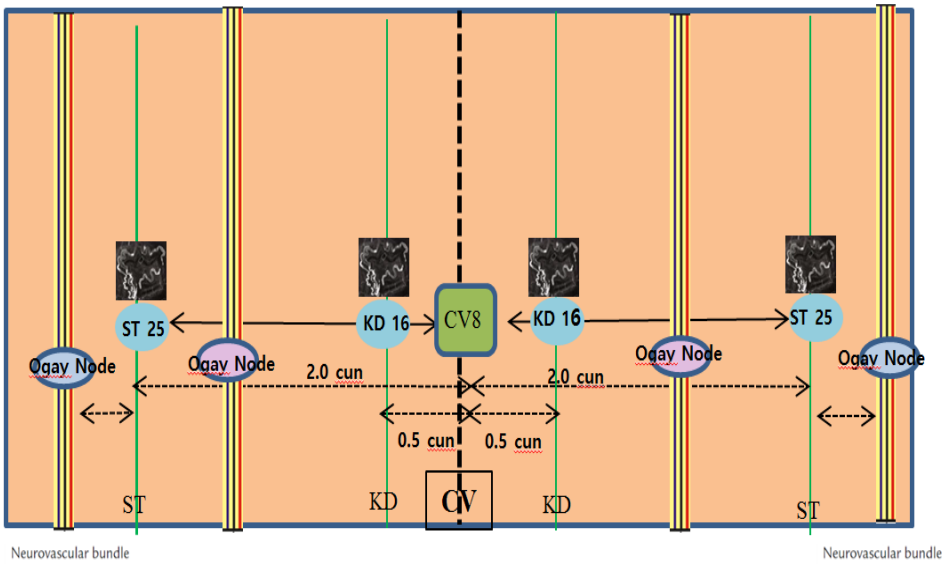

Fig 4.2.4. **<u>Illustration of neurovascular plexuses of coiled blood vessels along the kidney meridian (K) and stomach meridian (ST)</u>**

Which are 0.5 cun and 2.0 cun away from the conception vessel (CV). Pink oval shaped represent the ogay primo nodes found in three-day mouse model and light blue oval shaped represent the ogay primo nodes found in eight weeks mouse model. For more detailed study of neurovascular plexuses, they made immuno-fluorescence analysis with antibodies such as Lyve 1 (for lymph vessel), CD 31 (for blood vessels), 150 kDA, (nerve fibers) in previous study. This was very valuable resource used for this experiment. The morphometric description showed in figure 4.2.5 (B).

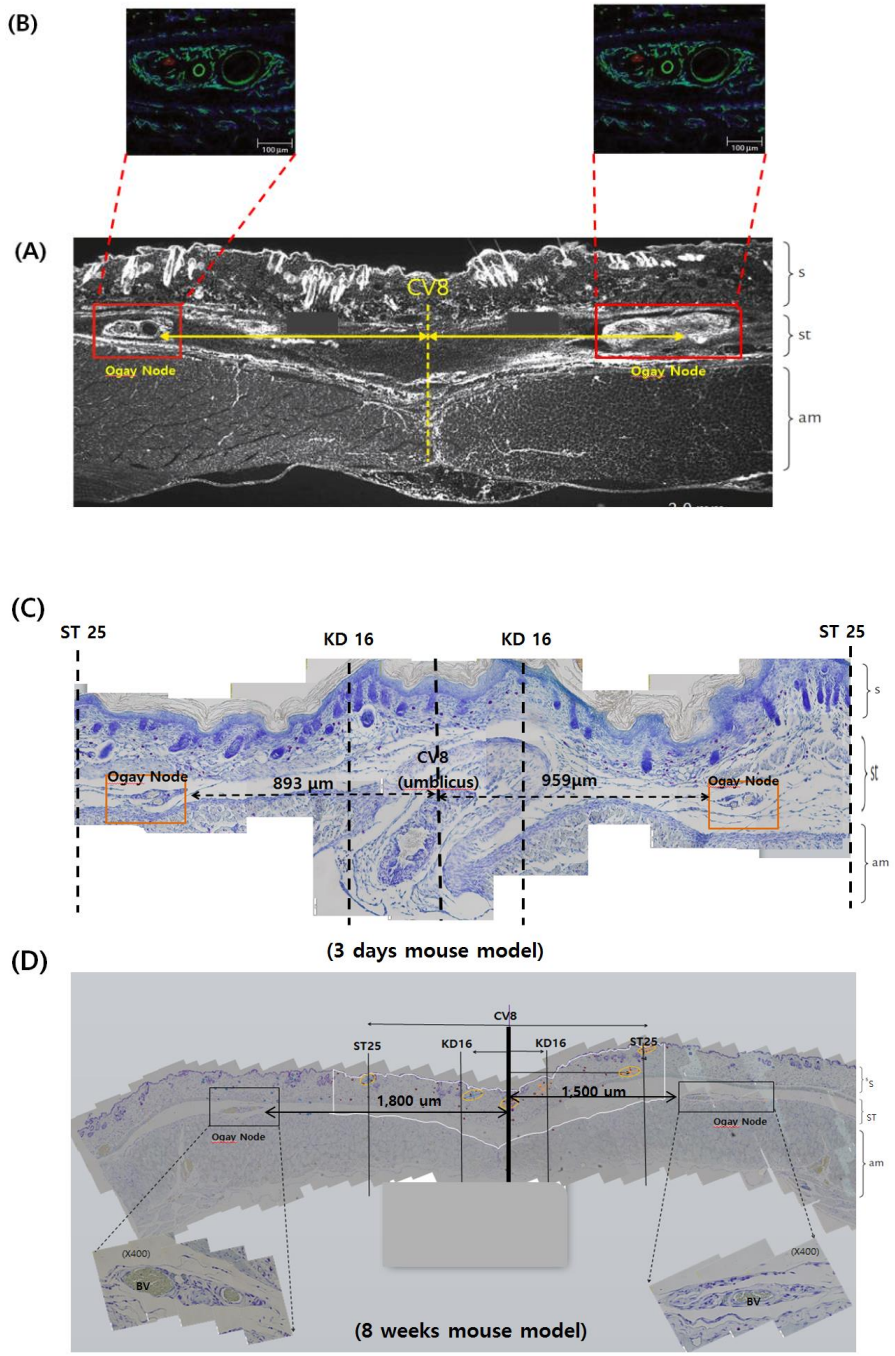

Fig.4.2.5. Images showing the anatomical location of ogay nodes

(neurovascular bundles) bilaterally in the abdomen skin sectioned. **(A)** Histological section of tissue shows the layers of skin (s),

Subcutaneous layer (st) and abdominal wall muscle (am) and the location of ogay nodes which are located under skin layer. **(B)** Magnified image of red rectangular box; transversal sectional view of the immunofluorescence imaging shows a typical neurovascular plexus including blood vessels, nerve fibers and lymphatic vessels. Green (CD31): blood vessel, Blue (Dapi): nuclei Red (150kDA): nerve fibers, and Bright Green (Lyve-1): lymphatic vessel. **(C)** 3 days model data: a histological section which stained with toluidine blue shows ogay node clearly. (*J Acupunct Meridian Stud 2009:2(1)*) **(D)** 8 weeks model data: a histological sectional view which stained with toluidine blue shows ogay primo node's location distinctively. The rectangular area of figure (D) shows the distribution of the nerve fibers, blood and lymphatic vessels in the neurovascular plexus.

According to Dr. Kim, a corpuscle (PN) founded in the skin is located mostly in the dermis layer, and there are many nerve endings, blood capillaries in it with mast cells. The corpuscle is connected by the primo vessel that runs into the muscle layer and the blood vessel bundles [2-20]. And his claimed theory is in agreed with the other scientist who does research on the APs in human. Here is one more observation in mice for different age groups also shared same idea with others about anatomical features of this structure.

Although in this work, we have shown the putative hypodermic PVS continued to 2009, however, we still cannot conclude our finding is the confirmation of APs as Kim's claim for the following reasons. First of all, it was not possible to visualize the PN in dermis layer which can be directly related to the APs due to limited method we use. In addition to that in order to be skin PNs, there are more detailed conditions has to be meeting as Kim described in his article. For example, in order to be a skin PN, it has to contain the small groups of chromaffin cells which located in the top part of inner

layer but unfortunately, we could not detect this in our specimens this time. And he stated that the most of skin primo node's head located in the dermis but ours are strangely located below hypodermis layer. And there are a few more criteria have to meet for the qualification. We can't be sure that ogay node is the one of the type of PN or APs or completely unknown structures. Those are the reasons why we need to plan for further studies for the confirmation. The finding the chromaffin cells may be a crucial to an unsolved problem whether the neurovascular plexus is the anatomical structure of the APs or Primo Nodes. Further studies must be followed to elucidate this question.

References

1. Ogay V, et al., “Observation of Coiled Blood Plexus in Rat Skin with Diffusive Light illumination”, *J Acupunct Meridian Stud* 2009; 2 (1): 56-65
2. Rabischong P et al., “experimentales de analgesia acupuncturale.” *Nouv Presse Med* 1975; 4:2021−6.
3. Bossy J. “Morphological data concerning the acupuncture points and channel network.” *Acupuncture Electrother Res* 1984; 9: 79−106.
4. Liu KY et al., “The correspondence between some motor points and acupuncture loci.” *Am J Chin Med* 1975; 3:347−58.
5. Gunn CC, et al., “Acupuncture loci: a proposal for their classification according to their relationship to known neural structures.” *Am J Chinese Med* 1976; 4:183−95.
6. Dung HC. “Acupuncture points of the cervical plexus.” *Am J Chin Med* 1984; 12:94−105.
7. Pan C, et al., “Moxibustion and Acupuncture Anesthesia. “In: *Research on Acupuncture*, Shang X, ed. New York: Springer-Verlag, 1988.
8. Shanghai Medical University, Human Anatomy Department, “A relationship between points of meridians and peripheral nerves: Acupuncture anesthetic theory study”. (People’s Republic Publishing House, Shanghai), 1973.
9. Ciczek LSW, et al., “Investigations of morphological structures of acupuncture points and meridians.” *J Trad Chin Med* 1985;5: 289−92.
10. Wang K, et al., “Needling sensation receptor of an acupoint supplied by the median nerve studies of their electro-physiological characteristics.” *Am J Chin Med* 1989; 17:145−55.
11. Heine H., “Funktionelle Morphologie der Akupunkturpunkte des Du Mai- und Ren Mai-Meridians”. *Dtsch Zschr Akup* 1990; 33:94−98. [In German]
12. Heine H., “Zur Morphologie der Akupunkturpunkte. *Dtsch Zschr Akup”* 1987; 30:75−79. [In German]

13. Heine H., “Functional anatomy of traditional Chinese acupuncture points.” *Acta Anat* 1995; 152:293.
14. Egerbacher M., “Veterinaerakupunktur. Anatomische und histologische Strunktur ausgewaehlter Akupunkturpunkte bei Rind und Hund. *Dtsch Zschr Akup* 1993; 36:75. [In German]
15. Draempehl D. et al., “Morphologische Untersuchungen a den Akupunkturpunkten Und meridianen bei Katzen und Hunden.” *Dtsch Zschr Akup* 1993; 36:104. [In German]
16. Zhang BZH., “Studies on the morphology and function of meridian lines with reference to neurogenic inflammation by ICR mouse. *Dtsch Zschr Akup* 1996; 39:29.
17. Stecco L., “La Manipalazione Neuroconnettivale.” (Editore marrapese, Roma) 1996.
18. Shanghai Medical University, Human Anatomy Department, A relationship between points of meridians and peripheral nerves: Acupuncture anesthetic theory study. (People’s Republic Publishing House, Shanghai), 1973.
19. Ciczek LSW et al., “Investigations of morphological structures of acupuncture points and meridians.” *J Trad Chin Med* 1985; 5:289−92.

4.3 Distribution of mast cells and Locations, Depths, and Sizes of the putative acupoints CV 8 and KI 16

4.3.1 Introduction

Mast cells (MCs) are active carriers of innate immunity against such conditions as allergies and inflammatory diseases [2, 3]. Therefore, the finding that the population of MCs is denser at APs and meridians than at nearby non-acupoints is not surprising [4, 5]; stimulation of the APs by using electro acupuncture or moxibustion has been found to induce degranulation of MCs [6–8]. This cytological characteristic of APs is in accordance with the recent finding that a particular tissue, called the primo node, in the primo vascular system (PVS) has a high population density of MCs [9].

In traditional Chinese medicine, the anatomical locations of APs can be identified by using the cun measurement method. However, dermal electrical impedance measurements do not significantly improve the precisions of those locations, and information on the depths from the epidermis and the sizes of the APs is totally lacking. Thus, in this work, we used the distributions of the MCs at three acupoints, the CV 8 and the left and the right KI 16 APs (fig 4.3.1), to estimate their locations, sizes, and depths from the epidermis. Knowledge of those parameters to submillimeter precision, along with knowledge of their cytological characteristics, would provide significant contributions to scientific investigations and to precise control of the practice of acupuncture.

Apart from acupuncture and the immune response, MCs synthesize, store, and release histamine and other mediators of inflammation [11, 12] and are crucial for the maintenance of tissue homeostasis, tissue repair, and the remodeling of the extracellular matrix [13, 14]. In addition, MCs accelerate epithelial-to-mesenchymal transitions, extracellular matrix degradation, and disease progression in some carcinomas [15]. Therefore, MCs are important cytological ingredients connecting western and eastern medicine [16].

In western medicine, the locations and the distributions of MCs have been studied in connection with their physiological functions. For instance, MCs are located at the host environment interface so as to initiate the host's defenses against intruders [17]. An early quantitative study on the distribution of MCs in normal mouse skin was performed by Larsson and Sylven to address the reactions of MCs to different chemical agents[18]. They developed a fairly reliable counting technique, but their study was limited to a small area of the dorsal skin, that is, an area on each side of the spine in the inter-scapular regions. They found that the numbers of MCs showed left-right symmetry in each individual, but the variations in the numbers of both dermal and hypodermal MCs between individuals were so large that the determination of an average standard number was not practicable.

The MCs of the skin lie in the dermis and the hypodermis, where they are grouped around blood vessels and nerves. A quantitative study on the association between MCs and blood vessels in human skin were first reported by Eady et al.[19]. They observed statistically significant correlations between MC counts and blood vessel counts in skin from the upper arm, but no similar correlations were observed in skin from the forearm. They also confirmed an uneven distribution of dermal MCs in human skin, which was consistent with the previous finding for mouse skin.

Although researchers noticed a highly-clumped distribution of dermal MCs with a population density that varied greatly within a small area encompassing a few mm^2 of skin [19], they did not recognize the relation between the regions of the skin with the clumped high density of MCs and the APs. Zhu et al. pointed out that higher densities of MCs were found at some APs compared with neighboring non-acupoints [4, 5]. MCs, blood vessels, and nerves were found to gather to form a complex at APs, and acupuncture stimuli were found to cause MCs to migrate to and be recruited in the APs and the meridians [20].

However, they compared the densities of MCs in the APs with those of unspecified non-acupoints rather than showing the distribution of MCs

throughout the skin. Therefore, the question of whether the densities of MCs in the skin could be used to get information on the locations, depths, and sizes of APs was not answered. Independently, the evidence for higher densities of MCs at APs was reinforced by a series of works on the abundance of MCs in the PVS in the abdominal cavity [21–23] and the abdominal wall [9]. This PVS prompted us to develop the current scheme of estimating the anatomical parameters for the APs in skin by making use of the distribution of MCs. Furthermore, a potential application of this anatomical information has already been proposed: the monitoring of the behaviors of APs during acupuncture treatment by measuring electroactive molecules, such as serotonin, secreted by granules of MCs [24].

Because of the significant roles of MCs, systematic investigations of the characteristics of their distributions in skin so as to extend the findings in previous works would be desirable [4, 5, 18, 19].

For this purpose, the number of MCs in a cross section of skin needs to be determined for the various APs. In this work, we examined a cross section of the abdominal wall. When we tried to observe a sectional view including several APs, we had to be certain not to miss the APs. We found that the APs could easily be missed because the precisions of the locations of the APs were only defined on the order of millimeters in terms of the F-cun method [25]; such a precision was too coarse for histological work involving sections with thicknesses of 5 to 10 μm. Because the umbilicus is one of the most well-defined points in the gross anatomy of abdominal skin and is known as conception vessel 8 (Shenque, CV 8), we chose it as the reference point for our histological work. As shown in figure 1, two other APs, the kidney 16 (Huangshu, KI 16) and the stomach 25 (Tianshu, ST 25) APs, are located at half F-cun and two F-cun, respectively, from CV 8 along the transversal line. Consequently, for our study, we chose a transverse section of the abdominal wall across the CV 8 acupoint.

4.3.2 Materials & Methods

4.3.2.1 Preparation and Sample Taking

For this investigation, 10 male 8-week-old ICR mice were obtained from Young Bio (Seoul, Korea). They were kept in an air-conditioned room at constant temperature and relative humidity (23 °C and 60%, resp.) with a 12-hour/12-hour natural light/dark cycle and ad libitum access to food and water. The animals were handled according to current international laws and policies (*Guide for the Care and Use of Laboratory Animals*, National Academy Press, 1996), and the care of the animals and the procedures used in this research were approved by the Institutional Ethics Committee of the Advanced Institute of Convergence Technology, Seoul National University.

The mice were anesthetized by using an intramuscular injection of a regimen consisting of 1.5 g/kg urethane and 20mg/ml xylazine. The volume of anesthesia administered to the mice was 0.04 ml. All surgery was performed under deep anesthesia and every effort was made to minimize suffering. The mice were sacrificed by over anesthetizing without any perfusion.

The anterior abdominal wall was removed from the mouse through an incision from immediately below the xiphoid cartilage to the bottom line of the urinary bladder so as to include either side of the right and the left superficial epigastric vessels bilaterally. We removed the specimen and washed it for an hour in tap water, after which it was immediately placed in 10% neutral buffered formalin (NBF) solution and stored for one day at room temperature. We also used a second fixative called orth solution, which contains potassium-dichromate. In this procedure, after orth fixation for a minimum of 24 hours, the specimens had to be stored in 70% ethyl alcohol (EtOH) until the surface of the specimen showed any signs of the orth-brown pigment.

After the fixation steps, we used a razor blade to remove the skin sample from a region ranging from about 500 μm above to 500 μm below the

umbilicus and sectioned it transversally to permit wider access to the regions of the CV 8 and the right and the left KI 16 APs bilaterally. These acupuncture points were determined based on the traditional finger-cun-measurement procedure corresponding to that for humans. All observations and operations were performed under a stereomicroscope (SZX12, Olympus, Japan).

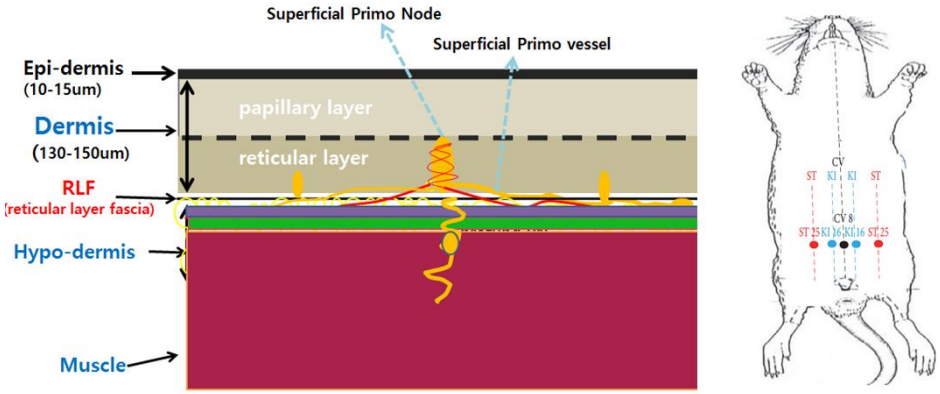

Fig.4.3.1 **Schematic illustration of acupoints along the meridian in the abodomen of a mouse**

(A) of imaginary superficial Primo node in skin layer.

(B) of acupoint along the meridian in the abdomen of a mouse. Three meridians, conception vessel (CV), kidney (KI) lines, and stomach (ST) lines, are shown. The acupoint CV 8 is located at the umbilicus.

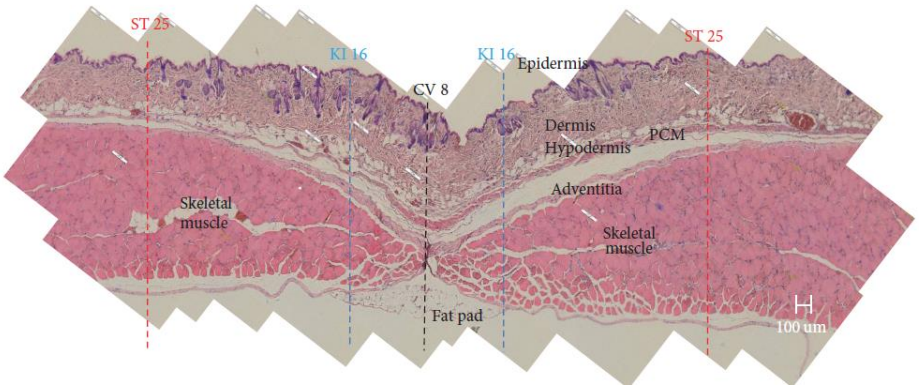

Fig.4.3.2. Cross-sectional image of a mouse abdomen showing its layers

Showing its layers (epidermis, dermis, hypodermis, panniculus carnosus muscle (PCM), adventitia, skeletal muscle, fascia, and fat pad). The traditional locations of acupoints are indicated with dotted lines.

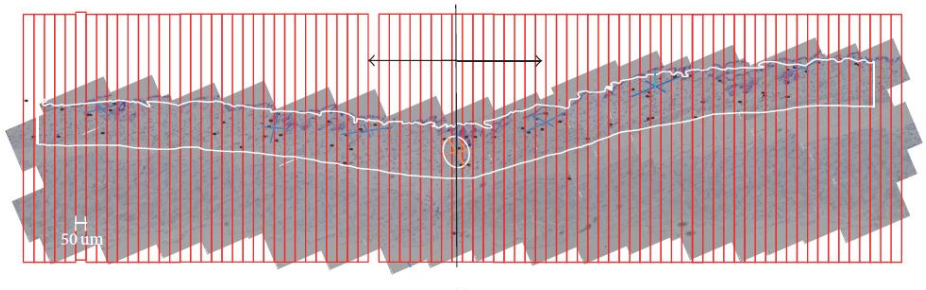

Fig.4.3.3. A toluidine-blue stained cross sectioned sample

A mesh of strips (50 μm each) in order to facilitate counting of MCs. The acupoint, CV 8 is indicated with an ellipse and the region of background is shown by the enclosing curve.

4.3.2.2 Staining

In the first fixing method, the isolated abdominal wall specimens were fixed immediately with NBF at 23 °C for 24hr ± 5 hr. The specimens gathered were processed in an automated tissue processor, after which they were embedded in paraffin wax. The resulting formalin-fixed paraffin-embedded blocks were cut into 5 μm thick sections by using a microtome (Reichert Jung 820, Leica, Germany). The sectioning continued until the search area, the middle parts of the umbilicus region (CV 8), had been reached. In the second fixing method, the isolated abdominal wall samples were immediately fixed with Orth's fixation solution at 23 °C for 24 hours while avoiding exposure to light. After fixation, the samples were washed in running water overnight and were then stored in 70% EtOH until use.

Two consecutive paraffin sections of 5 microns each from the search point were cut from the paraffin block. One was stained using the conventional hematoxylin and eosin (H&E) staining method (figure 4.3.2) and the other section was stained using the toluidine-blue staining method. We performed the H&E staining following a conventional procedure for the purpose of identifying the general histological features of the specimen. For the toluidine-blue staining, the toluidine blue stock solution was made by melting 0.1 gm of toluidine blue powder (toluidine-blue O, 198161-5G, Sigma-Aldrich, St. Louis, MO, USA) and 10ml of 70% alcohol. The working solution at pH 2.3 was made by mixing the stock solution with sodium chloride (1%, pH 2.3). The specimens were stained with toluidine-blue for 60 ± 20 sec. They were dehydrated by dipping them quickly 10 to 15 times first in 95% ethanol and then in 100% ethanol. They were then dipped in xylene for 3 minutes, after which they were mounted on a glass slide.

4.3.2.3 Counting of Mast Cells (MCs)

Finding the High-Density Area:

The stained specimens were observed under a phase contrast microscope (BX51, Olympus, Japan) to count the MCs, which were easily recognizable because of their stained red-purple (metachromatic staining) color and the background's blue color. The granules from the MCs, which were often scattered around the MCs, were a prominent signature of the MCs. As described by earlier researchers, the distribution of dermal MCs was uneven.

A mechanical calculation of the density of mast cells in dermal connective tissue could have easily led to an erroneous value because of various deformations of the skin, such as shrinkage and distortion, which occurred during the preparation of the sample [18, 19]. Therefore, the counting had to be defined specifically to fit the purpose of the work. In the present work, we divided the abdominal wall into three layers, as shown in figure 4.3.3. The 1st layer was the skin from the epidermis to the adventitia of the skeletal muscle. That layer included the dermis and the hypodermis, and the MCs were found to populate this skin layer mostly. The 2nd layer was from the adventitia to the fascia underneath the abdominal muscle. The 3rd layer was the fat tissue below the muscle layer. The fat tissue formed a pad directly below the umbilicus; MCs were also observed in that pad.

MC counts per length, instead of area, were considered by Larsson and Sylven as a practical way of density comparison [18], but we modified that method to apply a mesh of 50 μm strips to the sample, as shown in figure 4.3.3. These narrow strips helped experimenters to count the MCs correctly without missing any or over counting them. The MC counts of two consecutive 50 μm strips were recorded and presented graphically in figure 4.4 in the form of histograms.

4.3.2.4 Calculating the MC Number Density at the APs in the Skin and for the Background:

Having approximately found the high-density regions by using the histograms, we calculated more precisely the number density of MCs by measuring the area of each region by drawing, as shown in figure 4.3.5 an ellipse that covered the MCs. Instead of the density at non-acupoints, the overall background average density throughout the entire skin of the dermis and the hypodermis, excluding the high-density regions was calculated. For this, we used Image J and the TS View programs and counted the numbers of pixels. The size of a pixel was $0.64 \times 0.64\ \mu m^2$. The numbers of MCs, the areas of the high-density regions, and the number densities are presented in Table 4.3.1. The average density and other quantitative data were expressed as means ± standard deviations for ten animals. The locations of the putative APs, the CV 8 and the left and the right KI 16 APs, as determined from the densities of MCs, were given as the centers of the ellipses that covered the high-density areas. The locations, depths, and sizes of these putative APs are presented in Table 4.3.2. The average was taken over ten mice, and the standard deviations of the error are given.

4.3.3 Results

MCs were mostly distributed in the dermis and the hypodermis but were never found in the epidermis. Only very few MCs were observed near blood vessels below the hypodermis, that is, in the layers of the adventitia, skeletal muscle, and fascia. Surprisingly, MCs again occurred in the fat pad underneath the fascia, a finding that was not reported in previous studies [18, 19]. From the graphs in figure 4.3.4 showing the MC distributions, one can clearly see that the distributions are not even. From this gross feature of the distributions we selected regions that should be examined more closely. Figure 4.3.5 shows the five selected regions of abundant MCs.

We examined the locations of the high-density regions in connection with the three Aps, the CV 8 and the right and the left KI 16 Aps. In Table 4.7, we summarize data for the MC densities at the three putative Aps and for the background.

The average MC number densities were 3.3 ± 1.7/ (100 μm)^2, 2.7 ± 0.9/ (100 μm)^2, and 2.9 ± 0.9/ (100 μm)^2 at the CV 8 and the right and the left KI 16 acupoints, respectively, where we have used the practical and convenient unit of area for experimenters, that is, 100 μm × 100 μm. The MC number density of the background was 0.3 ± 0.1/ (100 μm)^2. The area and the MC density at the fat pad were 11.8 ± 9.9 × 104 μm^2 and 0.6 ± 0.5/ (100 μm)^2, the latter being about two times higher than the background density of the dermis and the hypodermis.

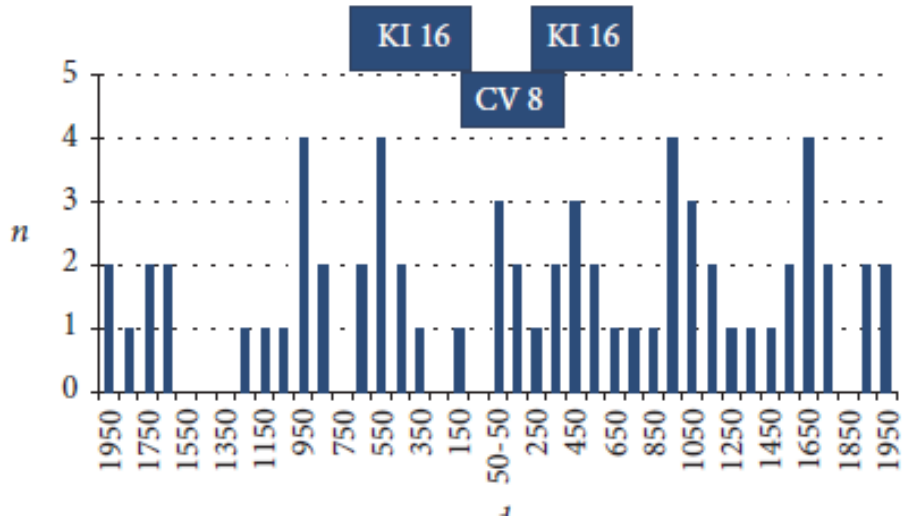

Fig. 4.3.4. **Graphical representation of MC density** (from figure 4.3)
X-axis (d) is the distance from CV8 in unit of μm. Y axis (n) is the number of MCs in 100 μm.

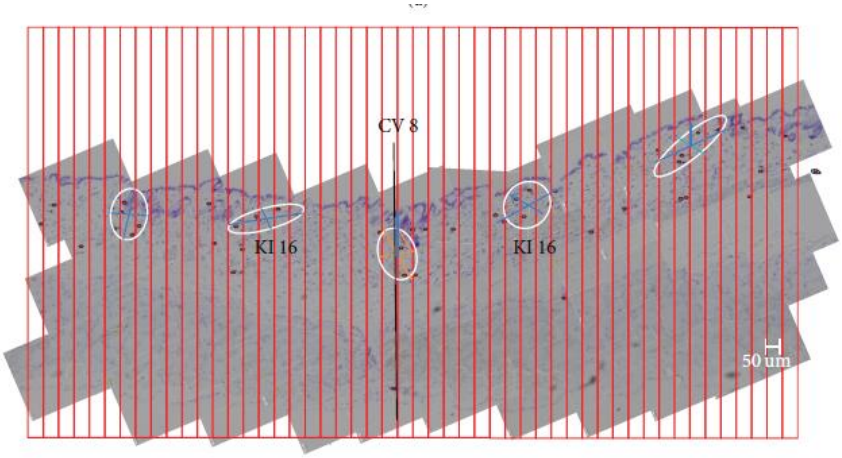

Fig. 4.3.5. **<u>The image of the selected five regions of high density of MCS with ellipses</u>**

The putative acupoints CV 8 and right and left KI 16 are indicated. Two more high-density points are also shown. They might correspond to ST 25.

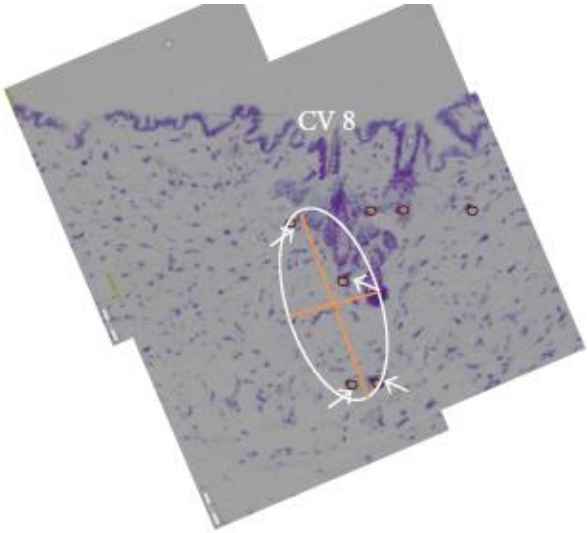

Fig. 4.3.6. **<u>A magnified view of the region of CV 8</u>**.

Four MCs are indicated with arrows. The center and the long and short axes of the covering ellipse are location and size of CV 8, respectively. The center lied in deep dermis below a hair follicle.

Table 1: Number density of mast cells at the putative acupoints CV 8 and KI 16 and at the fat pad and the background density.

M	A/W	CV 8			Right KI 16			Left KI 16			Right NHP			Left NHP			B			Fat pad		
		N	A	D	N	A	D	N	A	D	N	A	D	N	A	D	N	A	D	N	A	D
1	8/26	4	2.6	1.5	7	1.8	3.9	5	2.3	2.2	6	1.9	3.2	6	2.7	2.2	33	83.1	0.1	1	2.5	0.4
2	8/25	4	1.4	2.9	5	1.8	2.8	3	1.4	2.1	6	2.3	2.6	3	2.7	1.4	28	278.6	0.1	2	33.3	0.1
3	8/25	2	0.7	2.9	3	1.4	2.1	4	1.3	3.1	4	1.6	2.5	6	1.4	4.3	30	132.1	0.2	7	13.8	0.5
4	8/26	10	1.3	7.7	4	2.1	1.9	3	0.9	3.3	4	2	2	4	1.4	2.9	40	81.7	0.5	5	8.6	0.6
5	8/26	2	0.9	2.2	4	1.2	3.3	2	0.6	3.3	6	1.3	4.6	3	1.1	2.7	43	153.8	0.3	4	9.8	0.4
6	8/27	3	1.8	1.7	3	3.5	0.9	4	3.1	1.3	4	3	1.3	4	4	1	33	105.1	0.3	5	26.1	0.2
7	8/24	5	1.7	2.9	3	1	3	7	2.7	2.6	3	1.8	1.7	3	5.6	0.5	26	119.6	0.2	1	0.8	1.3
8	8/27	2	0.5	4	2	0.5	4	2	0.8	2.5	4	1.0	4	5	3.9	1.3	5	99.2	0.1	3	10.3	0.3
9	8/26	3	0.8	3.8	2	0.7	2.9	5	1	5	4	1.6	2.5	7	1.6	4.4	37	162.8	0.2	4	9	0.4
10	8/24	2	0.6	3.3	4	1.7	2.4	4	1.3	3.1	5	2.2	2.3	3	1.7	1.8	40	76.2	0.5	6	3.5	1.7
Average	8/25.6	3.7	1.2	3.3	3.7	1.6	2.7	3.9	1.5	2.9	4.6	1.9	2.7	4.4	2.6	2.3	31.5	129.2	0.3	3.8	11.8	0.6
SD	0/1.0	2.3	0.7	1.7	1.4	0.8	0.9	1.4	0.8	0.9	1.0	0.5	1.0	1.4	1.5	1.3	10.3	57.3	0.1	1.9	9.9	0.5

M = mouse number; A/W = age (week)/weight (g); NHP = next high MC density point; B = background; N = number of MCs; A = area (10^4 um^2); $D = N/A$ (number/10^4 μm).

Table 4.3.1. Number density of mast cells at the putative acupoints CV8 and two KI16 and at the fat pad

Table 2: Locations, depths, and sizes of the putative acupoints CV 8 and KI 16.

M	A/W	CV 8			Right KI 16			Left KI 16			Right NHP			Left NHP		
		X_c	Z	L/S	X	Z	L/S	X	Z	L/S	X	Z	L/S	X	Z	L/S
1	8/26	+114	250	283/117	416	177	208/113	443	88	245/119	964	133	233/105	883	164	293/118
2	8/25	−50	182	152/117	783	113	233/96	712	79	154/115	1467	383	258/115	1430	85	163/163
3	8/25	+17	25	128/67	450	129	203/89	550	194	167/100	1190	325	207/99	1767	258	144/128
4	8/26	+175	50	195/85	588	183	165/165	683	283	143/80	1523	250	218/119	1126	300	236/77
5	8/26	−67	133	133/83	356	64	180/82	318	137	90/86	922	112	149/111	1393	58	123/114
6	8/27	+50	317	228/98	483	233	275/163	580	67	220/179	1445	70	285/132	1617	233	250/202
7	8/24	+25	153	238/92	673	222	175/76	771	219	254/133	1634	171	174/132	1445	219	320/222
8	8/27	−44	290	116/60	888	220	83/83	738	111	137/73	1206	102	130/101	1208	109	265/187
9	8/26	−67	290	105/94	525	233	100/83	209	62	142/90	1188	112	208/99	939	56	183/110
10	8/24	+100	246	88/87	256	60	167/133	650	117	179/95	783	167	230/123	1251	200	214/102
Average	8/25.6	70.9	193.6	157.9/90	541.8	163.4	178.9/108.3	565.4	135.7	173.1/107	1232.2	182.5	209.2/113.6	1305.9	168.2	219.1/142.3
SD	0/1.0	44.9	97.0	62.1/17.5	184.8	64.2	54.2/32.2	178.4	69.7	49.4/29.8	268.5	98.5	45.1/12.1	266.5	82.7	61.9/45.7

M = mouse number; A/W = age (week)/weight (g).
X_c = distance from the navel (μm) in CV 8; X = distance from CV 8 to KI 16 acupoints and NHPs, respectively.
Z = depth from the epidermis (μm).
L/S = long axis/short axis of the covering ellipse (μm).

Table 4.3.2. Locations, depths, and sizes of the putative acupoints CV8 and two KI16

In Table 4.3.2, the locations, that is, the distances from the umbilicus, the depths from the epidermis, and the sizes of the long and the short axes of the three Aps are recorded. The distances from the CV 8 to the right and the left KI 16 Aps were 541.8 ± 184.8 μm and 565.4 ± 178.4 μm, respectively. The depths were 193.6 ± 97.0 μm, 163.4 ± 64.2 μm, and 135.7 ± 69.7 μm for the CV 8 and the right and the left KI 16 Aps, respectively. The centers of the Aps were mostly in the deep dermis and sometimes in the upper hypodermis. The average long axis × the short axis for the CV 8 AP was 157.9 ± 62.1 μm× 90.0 ± 17.5 μm. Similarly, for the right and the left KI 16 Aps, they were 178.9±54.2 μm×108.3±32.2 μm and 173.1 ± 49.4 × 107.0 ± 29.8 μm, respectively.

The region corresponding to the CV 8 AP is shown in Figure 4.3.7. The area and the MC count in it were 2.6 × 10^4 μm^2 and 4, respectively, giving a number density of 1.5/ (100 μm)^2. This region was enclosed by an ellipse with long and short axes of 283 μm and 117μm, respectively. This can be considered as a gross anatomical description of the putative CV 8 AP.

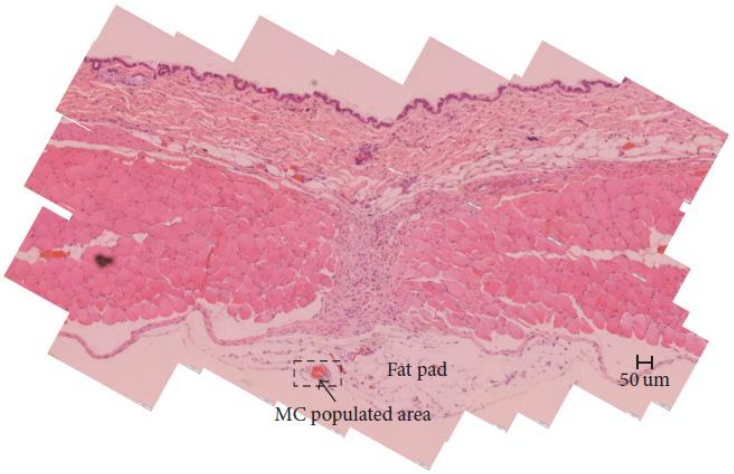

Fig. 4.3.7. <u>An H&E image showing the fat pad under the abdominal wall muscle.</u> **(**The MC populated region is indicated with a box).

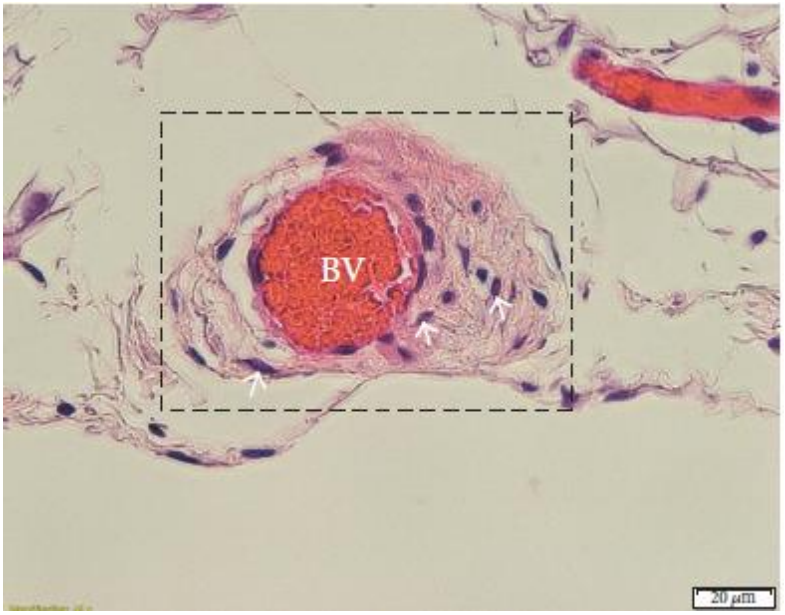

Fig.4.3.8. A magnified view of the MC populated Area

(Three MCs near a blood vessel (BV) are indicated with arrows)

Figure 4.3.8 shows a fat pad with a diameter. MCs were observed near the blood vessels in this fat pad. However, MCs of other mice were not in the similar location, sometimes being near the fascia and other times being near the parietal peritoneum. The distribution was not left-right symmetric either.

4.3.4 Discussion

Previous studies [4–8] on the relation between MCs and APs considered traditionally defined APS and they found higher densities of MCs at APs than neighboring non-APs. However, they did not investigate whether only APs have many MCs or there are non-APs which still have high density of MCs. Logically speaking, they found that the high MC density is a necessary condition of traditional APs but did not know whether it is also a sufficient condition. In this work, we found that it is not a sufficient condition

because there are many more points of high MC density compared to traditionally given APs. This new finding was possible because we investigated the MC distribution throughout the whole skin section, whereas previous studies examined only some preselected points. These high MC density non-APs raise new subjects for acupuncture study: whether they are hitherto unknown novel APs or merely accidental coincidences. If the former is right, MCs could be used to find new APs. If the latter holds, it remains to find the common factors that gather many MCs in APs and non-APs. In addition, and more importantly, our method of studying the MC density throughout the whole skin has the advantage of providing quantitative information about the locations, depths, and sizes of the APs up to the submillimeter scale which was not given in previous studies [4–8]. This cytological method is a newly developed tool which is useful for characterizing the APs together with conventionally used anatomical and histological methods [20, 25, 26].

Our results are in agreement with the first quantitative analysis of the distribution of MCs in the skin of a mouse by Larsson and Sylven [18], despite the uses of different strains of mice (ICR versus Swiss albino) and different locations. We studied the ventral skin near the umbilicus, while they studied the inter scapular regions of the dorsal skin. Both teams found a high density of MCs in the deep dermis and hypodermis, no MCs in the epidermis, and only very few in the adventitia, skeletal muscles, and fascia. These results are also consistent with data for the human arm [19].

In our case, the average background number density of MCs in the deep dermis and hypodermis for abdominal skin was $0.3 \pm 0.1/ (100\ \mu m)^2$. Larsson and Sylven reported that it was $2.4/ (100\ \mu m)^2$ in the dermis and $0.74/ (100\ \mu m)^2$ in the hypodermis [18]. Similarly, the MC density at non-acupoints near some APs of rats was reported to be $1.3 \sim 1.8/(100\ \mu m)^2$ [6]. In the case of human skin, Eady et al. reported $0.47/ (100\ \mu m)^2$ [19], and Craig and Schwarz quoted $0.31/ (100\ \mu m)^2$ in the dermis [27]. Large variations in the MC densities are known to exist, depending on the species, the individual, and

the location in the skin. When we consider the different histological processes, different positions, and individual variations in the various studies, we can conclude that our number densities are in reasonable agreement with those published elsewhere. In addition, a mechanical calculation of the density of mast cells in dermal connective tissue may easily lead to different values because of the various deformations of the skin which can occur during the preparation of the sample [18, 19]. Therefore, the density should not be taken as a precise standard average value, which may not even be definable.

Nevertheless, regions having clumped high densities of MCs, which are the putative APs, were consistently observed and were in accord with previous results for rats [4, 5]. In this study, the average MC number densities were 3.3 ± 1.7/ (100 μm)^2, 2.7 ± 0.9/ (100 μm)^2, and 2.9 ± 0.9/ (100 μm)^2 at the CV 8 and the right and the left KI 16 APs, respectively, which are in agreement with the data for rats: 2.3 ± 0.7 / (100 μm)^2 at ST 36, 2.4 ± 0.6 / (100 μm)^2 at ST 31, and 2.3 ± 0.6 / (100 μm)^2 at ST 25 [6].

In the current work, we were able to infer the locations, depths, and sizes of the three APs, CV 8 and the left and the right KI 16 APs, by making use of the number density of MCs. The MCs were all in the dermis and the hypodermis and had oval shapes with sizes of about 200 μm, as shown in Table 4.3.1. The distance of the CV8 AP from the umbilicus was 70.9 ± 44.9 μm. The distances of the right and the left KI 16 APs from CV 8 were 541.8 ± 184.8 μm and 565.4 ± 178.4 μm, respectively. These correspond to 0.4±0.1 F-cun. We used the F-cun measurement of finger width [25]. In our case, 1 F-cun was approximately 1.3mm. The F-cun measure of the KI 16 AP is 0.5 in traditional knowledge.

However, the regions highly populated with MCs did not always coincide with conventionally designated APs. For example, the next points from the KI 16 APs were only about 1,300 μm away from CV8, as shown in Table 4.3.2. If they were ST 25 as in traditional Chinese medicine, the distance should be about 2,600 μm. The extra high MC density point at 1,300 μm might be a novel extra AP which does not exist in a human body. If this is

true in general the MC density can be a novel cytological method to find extra APs. However, it might not be an AP at all. In this case, a subject to investigate in the future is the reason why some non-APs have high-density MCs. Currently the reason is not known either in traditional Chinese medicine or in western medicine.

One obvious limitation of the current work is the failure to determine the boundaries enclosing the APs by using the MC distribution. The reason was the limitation of the staining dye toluidine-blue that shows MCs well but cannot show many other components of the skin tissue. At the present time, the dye to stain the boundary cells or tissues of the APs is not known. For example, hema-color technique stained many other components of the primo node but it did not specifically show the boundary tissue [22]. So, it remains an important task to find the right dye to stain the boundary tissue of the APs, which we hope to solve in the future.

Interestingly, we found that rats and mice are different with respect to the fat tissue underneath the fascia. The fat pad of a mouse was a round or oval disk shape of about 1,000 μm in diameter (Figure 4.3.8). A rat has a long fat band, as compared to the fat pad of a mouse. Both the long fat band in a rat and the fat pad in a mouse are populated with MCs. The fat band of a rat has a PVS in it, and high densities of MCs in the PVS have recently been found in several works on the primo nodes in the abdominal cavity [9, 21–23].

The methods used in this study can be used to investigate the distributions of MCs for other skin areas to determine the gross anatomical features of APs. Similar studies on pathological conditions in mice will be useful for investigating the roles of MCs in the treatment of diseases. One medically significant application of nanotechnology to detect and monitor ST 36 by measuring the serotonin secreted by the MCs residing in the APs was proposed by Li et al. [24]. For this purpose, knowledge of both the locations and the depths of the APs, for which the current work provides useful information, are essential.

References

1. Son YS, et al., "Antipyretic effects of acupuncture on the lipopolysaccharide- induced fever and expression of interleukin-6 and interleukin-1β mRNAs in the hypothalamus of rats," *Neuroscience Letters*, vol. 319, no. 1, pp. 45–48, 2002.
2. Kalesnikoff J, et al., "Anti-inflammatory and immunosuppressive functions of mast cells," in Suppression and Regulation of Immune Responses, vol. 677 of *Methods in Molecular Biology*, pp. 207–220, Springer, 2011.
3. Theoharides T.C, et al., "Mast cells, mastocytosis, and related disorders," *The New England Journal of Medicine*, vol. 373, pp. 163–172, 2015.
4. Zhu Z, et al., "Morphometric observation on the mast cells under the acupuncture meridian lines," *Zhen Ci Yan Jiu*, vol. 15, pp. 157–158, 1990 (Chinese).
5. Zhong AM, et al., "Study of correlation between the mast cell and acupoint," *Shijie Zhenjiu Zazhi*, vol. 4, pp. 53–58, 1994 (Chinese).
6. Deng Y, et al., "Effects of electroacupuncture on the subcutaneous mast cells of zusanli acupoint in rat with unilateral sciatic nerve transection," *Zhen Ci Yan Jiu*, vol. 21, no. 3, pp. 46–49, 1996 (Chinese).
7. Deng Y, et al., "The influence of electro acupuncture on the mast cells in the acupoints in stomach meridian," *Zhen Ci Yan Jiu*, vol. 21, pp. 68–70, 1996 (Chinese).
8. Zhang D, et al., "Role of mast cells in acupuncture effect: a pilot study," *Explore*, vol. 4, no. 3, pp. 170–177, 2008.
9. Jang H, et al., "Observation of a flowing duct in the abdominal wall by using nanoparticles," *PLoS ONE*, vol. 11, no. 3, A.ID e0150423, 2016.
10. Kim BH, "The Kyungrak system," *J Jo Sun Med*, vol. 108, pp. 1–38, 1965.
11. Smith D.E, "The tissue mast cell," *International Review of Cytology*, vol. 14, pp. 327–386, 1963.
12. Lewis R.A, et al., "Non-respiratory functions of pulmonary cells: the mast cell," *Federation Proceedings*, vol. 36, no. 13, pp. 2676–2683, 1977.

13. Maurer M, et al., “What is the physiological function of mast cells?” *Experimental Dermatology*, vol. 12, no. 6, pp. 886–886, 2003.
14. Noli C, et al., “The mast cell in wound healing,” *Veterinary Dermatology*, vol. 12, no. 6, pp. 303–313, 2001.
15. Johnson C, et al., “Inhibition of mast cell-derived histamine decreases human cholangiocarcinoma growth and differentiation *via* c-Kit/stem cell factor-dependent signaling,” *The American Journal of Pathology*, vol. 186, no. 1, pp. 123–133, 2016.
16. Fung P.C.W, “Probing the mystery of Chinese medicine meridian channels with special emphasis on the connective tissue interstitial fluid system, mechano transduction, cells durotaxis and mast cell degranulation,” *Chinese Medicine*, vol. 4, article 10, 6 pages, 2009.
17. Metcalfe D.D, et al., “Mast cells,” *Physiological Reviews*, vol. 77, no. 4, pp. 1033–1079, 1997.
18. Larsson L.G, et al., “The mast cell reaction of mouse skin to some organic chemicals I. Estimation of the relative number of mast cells in normal mouse skin,” *Cancer Research*, vol. 7, no. 11, pp. 676–679, 1947.
19. Eady R.A, et al., “Mast cell population density, blood vessel density and histamine content of normal human skin,” *British Journal of Dermatology*, vol. 100, pp. 623–633, 1979.
20. Mingfu L, et al., “Study on the dynamic compound structure composed of mast cells, blood vessels, and nerves in rat acupoint,” *Evidence-based Complementary and Alternative Medicine*, vol. 2013, Article ID 160651, 4 pages, 2013.
21. Kwon BS, et al., “Microscopic nodes and ducts inside lymphatics and on the surface of internal organs are rich in granulocytes and secretory granules,” *Cytokine*, vol. 60, no. 2, pp. 587–592, 2012.
22. Lim CJ, et al., “Identification of primo vascular system in abdominal subcutaneous tissue layer of rats,” *Evidence-Based Complementary and Alternative Medicine*, vol. 2015, Article ID 751937, 13 pages, 2015.
23. Gil HJ, et al., “Number density of mast cells in the primo nodes of rats,”

Journal of Acupuncture and Meridian Studies, vol. 8, no. 6, pp. 288–293, 2015.

24. Li Y, et al., "In vivo monitoring of serotonin by nanomaterial functionalized acupuncture needle," *Scientific Reports*, vol. 6, no. 1, A. ID 28018, 2016.
25. World Health Organization, *WHO Standard Acupuncture Point Locations in the Western Pacific Region*, World Health Organization, Geneva, Switzerland, 2008.
26. Langevin HM, et al., "Relationship of acupuncture points and meridians to connective tissue planes," *The Anatomical Record*, vol. 269, no. 6, pp. 257–265, 2002.
27. Craig SS, et al., "Tryptase and chymase, markers of distinct types of human mast cells," *Immunologic Research*, vol. 8, no. 2, pp. 130–148, 1989

Chapter 5

5.1 SKIN Chromaffin Cell Study

5.2 Medical Application of PVS

Chapter 5

5.1 Skin Chromaffin Cell Study

5.1.1 Introduction

To understand the nature of APs and its mechanism, many researchers have tried to search for distinct anatomical and histological features that could differentiate APs from the surroundings.

Unfortunately, in a preliminary report based on our observation of similar morphological features of superficial skin PN' in post-natal 3 days old mice model, we did not succeed in observing the chromaffin cell in the inner substance part of putative primo node (AP) in the skin due to our limited method. Therefore, in this chapter I would like to share the information we got through this experiment.

Visualization of this characteristic cells which may give us a key for clear distinction from the neurovascular bundles (possible candidate of putative AP or PN) or totally different unknown structure.

As founder Kim described that histological investigations of acupuncture points (APs or S-PN) in the skin have revealed a number of characteristic properties such as a specific distribution of well-developed blood vessel networks inter-connected with the nerves [5,6], a high density of nerve endings [1-4], a gathering of mast cells around a blood plexus [7,8]. Many researchers from China, France, Germany, etc. have been studied the relationship between acupoints (S-PN) and the surround connective tissues however, until now, no one has been provided the evidence corresponding APs and meridians except for his findings. [9] Chromaffin cell terms used to designate catecholamine-containing elements that are neuro-ectodermal in origin and innervated [14].

APs have been reported to have a high concentration of catecholamine's in comparison with non-APs in the skin, and, thus, our team has tried to examine the presence of chromaffin cells associated with mouse APs [9]. Thus, we focused to find the chromaffin cells which located in the inner substance's upper and middle parts of S-PN (fig 5.1.1 (A) & (B)) and developing a method to identify this easily in this work. Compared to the chromaffin cells that we can see in the medullar of adrenal gland, the skin chromaffin cells have its own distinct characteristics. The first chromaffin cells in the skin form the small number of groups and distributed in rows in the inner layer part of S-PN and second, the many blood vessels were distributed around to it and lastly, its size was described to be diverse in form. Usual size is about 15-25 um in diameter and its shape being round or oval (fig 5.1.2) [10].

More to the points above, these cells are one of the cell groups which contain the special granules. The chromaffin granules in these particular cells were associated with release of vasopressor substance such as catecholamine, dopamine, adrenalin and noradrenalin and a variety of another neuropeptide. Among them, especially the catecholamines are known to be released by chromaffin cells in situations of stress. [9] The special granules inside these are obscure in most cases, and sometimes, it has undergone the transition of chromaffin granules to basophile granules in the sinus of the S-PN (fig 5.1.2). According to Kim, the granules are easily scattered around the blood capillaries in the inner substance of PN and it was visualized by the technique of modified giemsa staining (old name was sevki staining) after the old fixation method.

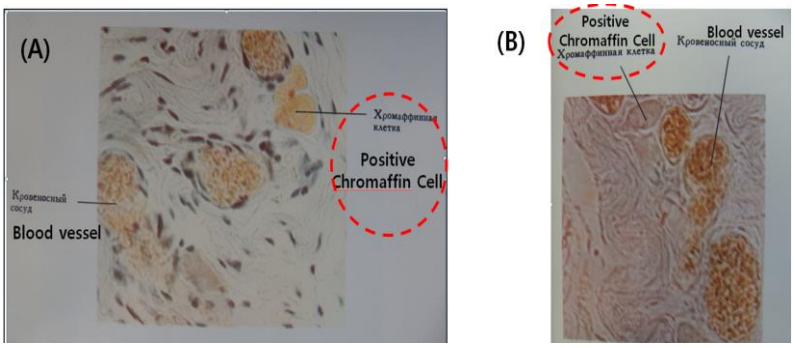

Fig.5.1.1 **Chromaffin Cells detected in sinus.**

(A)BH Kim's picture showing that chromaffin cells found inside of superficial primo node (S-PN). **(B)**An image showing that chromaffin cell revealed under the sevki staining by positive reaction with granules inside of S-PN (from *Bonghan Kim's 1st article*)

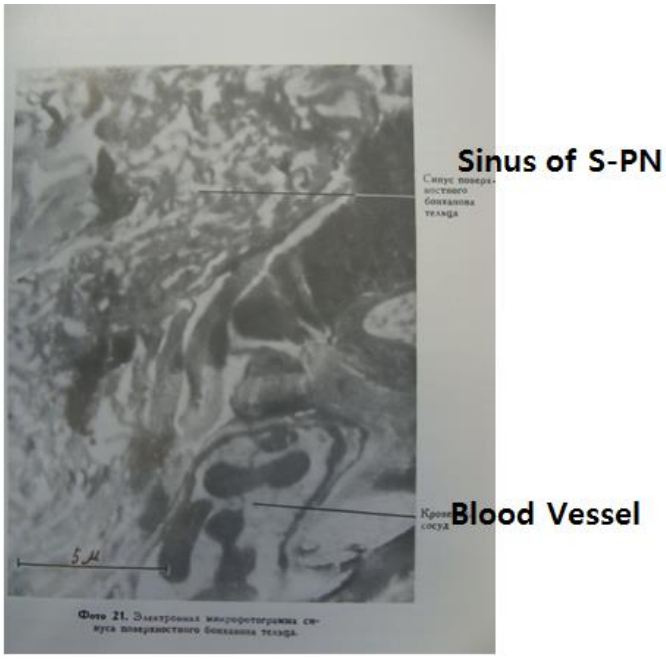

Fig.5.1.2 **Electron micrograph of the sinus of superficial primo node**

(from *Bonghan Kim's 1st article*)

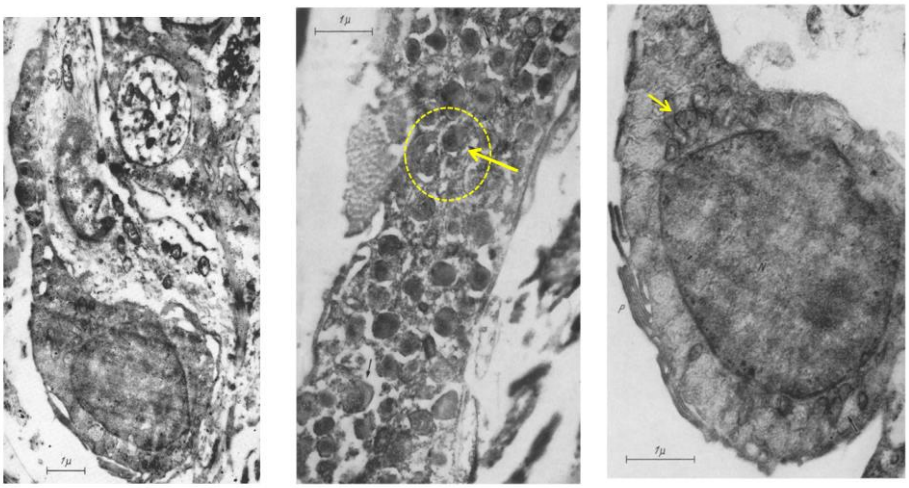

(A) (B) (C)

Fig.5.1.3 **Electron micrograph showing chromaffin cells**

(A) With its typical shape: the thickening around the nucleus and the tail-like extension of the cytoplasm. The lighter, connected cells are fibroblasts. (Magnification: x13, 000) **(B)** The chromaffin grannies have a mean diameter of about 0.35 micron with a centerelly located. Body, the size of which is about 0.2 um, especially well seen at arrows. (Magnification: x 28,800) **(C)** The surface of the chromaffin cell, especially the part corresponding to the location of the nucleus (N) is fitted with long and narrow projections (P). Groups of mitochondria are seen in the vicinity of the nucleus. (Magnification: 24,400) (*Circulation Research, Volume Vi, July 1958*)

The method described in old published papers related to find chromaffin cells are those that are not currently used. So, we spent a lot of time looking for specialized staining technique and old fixation method. From what we learned from the previous study these cells usually stained by chromium salt staining and in order to achieve the good standing of staining,

we had to change the method of sample fixation. These have become a lot of challenges. Thus, we want to briefly explain the experiment methods we have found for the next researchers

5.1.2 Materials & Methods

5.1.2.1 Animals

Aged 8 weeks of balb/c mice in both sexes were obtained from the Doo Yeol Laboratory Animal Company (Seoul, Korea). The animals were housed in a constant temperature-controlled environment (23°C) with 60% relative humidity. All animals were anesthetized with a mouse cocktail solution, a mixture of saline, zoletil and rompun.

5.1.2.2 Fixation Solution Preparation

This fixation solution is used for the demonstration of chromaffin granules in the skin. But it is not a good general-purpose fixative. The chromaffin granules are colored light orange to brown by chromate; the reaction is most intense at pH of 5 to 6. For the mixture, it requires to make stock solution first with potassium dichromate, sodium sulfate, and distilled water. Mix the stock solution with formaldehyde to make working solution. But Formaldehyde must add just before use and mix. It has a corrosive nature so it always has to be handling with care.

5.1.2.3 Tissue Fixation and Embedding

Especially, in order to observe the skin chromaffin (chromate-loving) cell and granules, we had to use the specially made fixation solution that is Orth's fixation solution. Conventional use of PFA 4% does not a good purpose fixative to observe in these cells. In principle, the chromaffin granules are colored orange to brown by chromate salts, and the reaction is readily occurred at a pH of 5 to 6. Fix the specimen in Orth's solution for 24-

48 hours but due to its corrosive and carcinogen nature, it should handle with care. After the fixation, the specimen must be washed in running water until the all the brown pigments are gone in the skin and it takes quiet a time. After this process, the specimen was embedded in paraffin and sectioned as usual. As we explained, the Orth's fixation solution was very common to use in 1960s but not in use these days. When we ask for this method to the expert, no one has known this so at the end of many failures, we finally find a recipe of this product.

5.1.2.4 Sample Preparation

Specimens of skin were taken from the mouse abdominal cavity. In the specimen, CV line was contained with marked the putative acupoints of CV8, KD 16 and ST 25. Cut the specimen with a micro scissors and a razor and immediately fixed this sample in Orth fixatives solution at least 24 hours in dark room. This solution is very light sensitive so it should be avoided from direct sunlight.

5.1.2.5 Chromaffin granules Staining Methods

The fine and coarse granules in chromaffin cell is filled evenly in the cytoplasm and these granules stained yellowish brown by dichromate (chromate salt) due to the positive reaction [11]. In old method, they just use one method called sevki staining but through our test, there are other staining methods applicable to detect these cells. Here is the list which could be identified by the various staining method under the orth fixation. The following histological stains were used in this experiment.

1. Azo-coupling reaction in alkaline solution. Gomori's method with 2-amino-5-azo toluol was used. For this staining, the specimen was fixed partly in orth's solution and partly in formalin.

2. Modified Sevki (Modified Giemsa) method: with modified Sevki method, chromaffin granules in the skin should react positively and stained granules in the color of light to dark brown color.

   Steps: After application of a modified Sedki stain (modification will be needed but usually 2 drops of Giemsa's solution per millimeter of distilled water for 2 hours at 50°C), the specimen was rinsed in distilled water and differentiated, under microscopic guidance, first in a 70% solution of ethyl alcohol, then in a 90%, a 95%, absolute alcohol, and finally xylene. (*circulation Research*, *volume VI, July 1958*)

Staining Method	Chromaffin Cell	Mast cells
Gomori	purplish red	--------
M. Giemsa	**A**: bluish purple (Basophile granules: blue)	Reddish purple
	Non-A: pink	

(A)

Staining Method	Chromaffin Cell	Mast cells
M. Giemsa	**A**: yellowish brown (Basophile granules: blue)	Reddish purple
	Non-A: greenish blue	

(B)

Fig.5.1.4 **The color chart of cells different staining methods**

(A) Fixed in formaldehyde based fixative used

(**B)** Fixed in formol-dichromate based fixative used. In this case, chromaffin cells stained the cells show the same color described in Kim's paper.

In the skin, there are other cells containing granules in addition to the chromaffin cells (figure 5.1.4 (A) & (B)). The most of granular cells can be

found in the dermis layer of the skin is the mast cells (MCs). But by their granule sizes, it can be easily distinguished the type of cells. For example, the MCs did not contain chromaffin positive granules and in size, chromaffin granules are bigger than MCs granules (0.2-0.3um). In figure 5.1.4 shows that even types of chromaffin granules (epinephrine (A) or non-epinephrine (Non-A)) can be distinguishable in different colors. For the additional tip, the 85% of chromaffin cells are contained epinephrine secreting granules in mouse this could help which color we have to look for to identify these.

Chromaffin reacting cells were irregularly distributed among collagen fibers in the dermis of the skin and of other organs as well, more predominate in the vicinity of blood vessels, nerves, hair follicles and sebaceous glands [14] by pre-ganglionic sympathetic nerve fibers.

The modified Giemsa stain known to stain chromaffin tissue but not specifically for it, was employed to show cellular details more clearly [12]. And when this method applied to chromated tissue produces a greenish brown color in the presence of adrenalin or noradrenalin [14].

In this present work, we could not have confirmed the existence of chromaffin cells in skin layer however, as we emphasized many times, finding the further evidence to support the presence of chromaffin cells is very crucial. Since all methods used to demonstrate these cells here in this work are not specific, therefore it must be developed further methods to confirm directly by histochemical approach. Finding the presence of chromaffin cells in skin can change the paradigm of oriental medicine.

References

1. Zhang K, et al. “A morphological study on the receptors of acupuncture points.” *J Tradit Chin Med* 1982; 2: 251−60.
2. Tao ZL, “The progress of the morphological research on the acupoint.” *Zhen Ci Yan Jui* 1989; 14:397−402.
3. Wick F, et al. “Morphological analysis of human acupuncture points through immunohistochemistry.” *Am JPhys Med Rehabil* 2007; 86:7−11.
4. Li AH, et al., “Human acupuncture points mapped in rats are associated with excitable muscle/skin-nerve complexes with enriched nerve endings.” *Brain Res* 2004; 1012:154-9
5. Lu GW, “Characteristics of afferent fiber innervation on acupuncture points Zusanli.” *Am J Physiology* 1983; 245: R606−12.
6. Ciszek M, et al., “Investigations of morphological structure of acupuncture points and meridians.” *J Tradit Chin Med* 1985; 5:289−92.
7. Hwang YC., “Anatomy and classification of acupoints.” *ProblVet Med* 1992; 4:12−5.
8. Beng Y, et al, “The influence of electroacupuncture on the mast cells in the acupoints of the stomach meridian.” *Zhen Ci Yan Jiu* 1996; 21:68−70.
9. Ogay V, et al., “catecholamine-storing Cells at Acupuncture Points of Rabbits.” J Acupunct Meridian Stud 2008; 1(2):83-90.
10. Nordenstam H, et al., “Chromaffin Granules and Their Cellular Location In human skin.”, Zeitschrift fur Zellforschung, Bd. 45, S. 435-443 (1957)
11. Kim BH. “Study on the reality of acupuncture meridians”, *J Jo Sun Med* 1962; 9: 5−13.
12. Phillips J.H, et al., “Significance of Tissue Chromaffin Cells and mast Cells in Man”, *Circulation Research*, Volume VIII, July 1960
13. Matz L.R, et al, “Staining Characteristics of chromaffin granules in human skin”, *Nature* volume 194, May 12 1962
14. Burch G.E, et al., “Chromaffin Reacting Cells in Human Digital Skin”, *Circulation Research*, Volume VI, July 1958

15. Kim BH. “On the acupuncture meridian system”, *J Jo Sun Med* 1963; 90: 6−35.
16. Kellner G. Bau und Funktion der Haut. *Deutsh Z Akupunkt* 1966; 15:1−31.
17. Hu XL. “Modern scientific research in acupuncture channels and collaterals in traditional Chinese medicine. People’s Hygiene Publish House, Beijing, 1990.
18. Bensoussan A. “*The vital meridian. A modern exploration of acupuncture*”, Churchill Livingstone, Melbourne, 1991

5.2 Medical Application of PVS

5.2.1 Third Circulatory System may offer a cure for incurable diseases?

The primo vascular system extends throughout the brain, spine, and nervous system and due to its role in regeneration; we could carefully presume that PVS will play a key role in the development of many types of health conditions. [6] Then next question will be about how and under what condition it will involve in. There are still many important questions remaining to be answered in the part of (1) understanding the physiological roles of the PVS (during pre-birth, development and growth, and aging), (2) the roles of PVS in diseases including metabolic disease such as cardiovascular diseases, and diseases of central nervous system, (3) the formation of primo-microcells and their functions in regenerations, and (4) relations between the effects of PVS stimulation and acupuncture therapy [11].

Use the fact that PVS's circulation capacity and in vivo existence throughout the whole body, it could tell us a hint how it playing a role in our body fighting against in many types of intractable diseases such as cancer, Alzheimer and Lou Gehrig's disease. That is why this system has been widely recognized as a creative area for future regenerative medicine. The PVS solves many problems of modern medicine. In this chapter, the medical significance of PVS will be introduced with examples.

5.2.2 Cancer

Although many studies and treatments for cancer have been introduced so far, there are still no perfect answers to its origin and mechanism. With these questions, we started the experiment and were able to suggest a few possibilities. From the previous experiments, we have been identified that the primo vascular system is densely populated in and around

tumors. Usually it is not densely populated except for the adipose tissue [6, 9]. What does this mean to us? The possible explanation would be that PVS could serve as a third pathway of cancer metastasis that could be blocked off in order to slow or stop the spread of cancer [9]. Therefore, it might be very important to point out the relationship between the cancer progression and formation of PVS.

In the previous studies, as a proof of the hypothesis, we have been showing the roles of the PVS in cancer cell transport via the cancer PVs, and confirmed that by tracing the QDs contained cancer cells [10]. Also, another study also confirmed that cancer induces dense PVS formation in close proximity to cancerous tumors, which suggests that a cancerous environment triggers cancer PVS formation [9].

The relationship between the cancer progression and the cancer PVS formation / cancer cell transportation via the cancer PV is a new founding but very important and deserves immediate attention for more complete understanding to develop novel tools for cancer prevention, diagnostic, and treatment. The cancer PVS may have a very important impact in cancer metastasis and if it is a common signature of cancer, then it may be utilized for early detection of cancer [9].

Another significant finding with the Trypan blue staining technique allowed us to discover the PVS on the fascia of cancer tissues. After subcutaneous inoculation with human lung cancer cells, the tissues were grown in the skin of nude mice for observation of changes occurring. The Trypan blue staining revealed a visualization of the PVS connected to tumor tissues [12]. The intraperitoneal inoculation case, the PVS was connected to tumor tissues grown in internal organs [10]. These results elucidate that the possible application of PVS as a drug delivery path for cancer.

It is therefore logical to conclude that the cause of cancer might be the pathological change of PVS however, in order to answer to the remaining questions systematically, future studies towards cancer need to be explore the facts and details at least three potential directions in 1) PVS as a potential

conduit for cancer cell metastasis, 2) PVS as a new route for drug delivery, 3) study of the relation between the PVS and the immune system [11].

5.2.3 Alzheimer Disease

Alzheimer's disease (AD) is a chronic neurodegenerative disease that usually starts slowly and worsens over time [1, 2]. It is the most common cause of dementia in order people and accounts for 60% ~80% of cases [3]. So far, no treatments stop or reverse its progression, though some may temporarily improve symptoms [2]. Affected people increasingly rely on alternative medicine hoping that such treatments might produce improvements in quality of life and delay cognitive decline [4.5]. Also, dementia, and specifically Alzheimer's disease, may be among the most costly diseases in these days.

Again, AD is a large part of the geriatric disease and in other words, mostly it can say that it is an aging related disease. Age-related diseases are organ damage due to people becoming older and living longer and longer. Those diseases can best be dealt with by a tissue regenerating system. This regeneration system may be the one of the main functions in primo vascular system due to that reason, if we know the PVS and primo microcell (sanal)'s relationship thoroughly, the system can be manipulated to lend a greater hand in healing such diseases. Therefore, it is very crucial to understand this system.

To identify the facts, cause this, it will be necessary to examine various parts in our body. The primary areas to focus on related to PVS regarding to this will be the parts relating to biomaterials and tissue engineering [6].

As we explained previous chapters, P-Vessels carry hormones and immune cells and play a key role in natural body regeneration. What exactly does it mean? If we can determine the role of P-fluid & P-microcells in physiological functions such as immune function and regeneration will give

us a big clue to develop entirely new diagnoses and treatment methods.

With regards to the immune function, the immune system is generally known to be a system of biological structures and processes that protect the body from many types of pathogens [6]. In PVS, according to Dr. Kim's, primo fluid carries different types of immune cells and the primo systems is still an unknown field of the immune system that will provide entirely new treatment protocols to us. In addition to that, the tissue engineering and biomaterials allow for the growth of new body tissues and organs from damaged state. Research will need to focus towards the fact that how the primo vascular system influences and regulates tissue growth. As we are able to assume that the P-system is responsible for regeneration, this may be the missing factor that explains some of the unpredictability in reliably initiating and controlling the growth of replacement tissue and organs [6].

At present, there is no definitive evidence to support that any particular measure is effective in preventing AD and clearly, more investigations are required [7]. We do not yet provide a clear treatment method of Alzheimer's at this moment but we are wondering that if we can link the mechanism of the body with the roles of PVS, we might get a step closer to develop new methods for diagnosis and treatment of this incurable health conditions from the new aspects. It will have a huge impact on existing theory and change a paradigm of treatment protocols in many malignant health conditions.

5.2.4 Stem Cell

With accelerating development of modern technology, the growing demand for healthy lives and the treatment of diseases is growing very high. Nevertheless, there are a number of problems that lead to chronic problems such as spinal cord injury, brain diseases, and intractable diseases. Stem cell therapy is a new treatment method which reflects people's need

Dr. Kim described in his article that primo microcells carry DNA

granules, proliferate in culture, can freely move in PVS system, regenerate injured tissue, and overall behave as multipotent stem cells [13, 14]. Aspects of stem cell research, PVS research needs to focus on analyzing primo microcells as well as identifying its role in the body and, moreover, the relationship to stem cells and very small embryonic stem cells (VSEL) [6]. The primo microcells (0.8 - 2.4 um in diameter) could prove to be a very important key in understanding and utilizing stem cells [6].

At this point in time, we are mainly focusing on developing technologies for detecting and analyzing neuro-primo system networks widespread within the body and identifying homing pathways of mesenchymal stromal cells (MSCs) through the injection on specific acupuncture point (presumed to be PN) which has been known for its disease preventability together. In order to prove the theory, repeated confirmation of the results by specifying the moving path of the injecting cells is required. When this experimental technology is set, it could offer a glimmer of hope on investigation of treatment mechanism based upon oriental medicine theory for neural diseases. Moreover, this step of research has a significant meaning in finding effective drug delivery pathways at targeting area with lowering the chance of side effects. This step of research has a significant meaning in finding effective drug delivery pathways at targeting area with lowering the chance of side effects. Even though this research is an ongoing topic, still there are many limitations exist and difficult to consider all the potential implications.

To sum up briefly in circulatory system, the primo vascular system is an essential component [13], together with lymphatic and blood circulatory system. PVS is extended throughout whole body, inside and outside of vessels, over the various organs, in the skin and the peripheral nervous system [14]. In other words, the PVS has unlimited potential to use in medical field and opens novel possibilities of integral medicine. Therefore, it is very important to focus on well-planned research based on the advanced biotechnology to find out the available points.

References

1. Burns A, et al., "Alzheimer's disease*", The BMJ*. 338*: b158. February 2009*
2. "Dementia Fact Sheet N°362", World Health Organization. March 2015. Archived from the original on 18 March 2015. Retrieved 13 January 2016.
3. Alzheimer's Association. "Alzheimer's Disease Facts and Figures", October 2008.
4. Diamond B, et al., "Complementary and alternative medicines in the treatment of dementia: an evidence-based review", *Drugs Aging* 2003; 20: 981-998.
5. Pope SK, et al., "Complementary and alternative therapies for Alzheimer's disease: a conference summary", *Alzheimer's Care Q* 2006; 7 13-31
6. Potroz M, et al., "Primo Vascular System: Basic and Applied Research Outline", The Primo Vascular System: Its Role in Cancer and Regeneration. Springer Science + Business Media pp 41-46.
7. "Systematic Review of Information and Support Interventions for Caregivers of People with Dementia", *BMC Geriatrics*. 2007; 7: 18.
8. Kawas CH. "Medications and Diet: Protective Factors for AD". *Alzheimer Disease and Associated Disorders.* 2006; 20(3 Supple 2): S89–96.
9. Kang KA, et al., "Primo Vascular System and Its Potential Role in Cancer Metastasis", *Oxygen Transport to Tissue XXXV*, Advances in Experimental medicine and Biology 789, Springer Science + Business Media, 2013; pp 289-296
10. Yoo JS, et al., "Characterization of the primo-vascular system in the abdominal cavity of the lung cancer mouse model and its differences from the lymphatic system. *PLoS One* 5(4): e9940

11. Harrison DK, et al., “The Primo Vascular System: Facts, Open Questions, and Future Perspectives”, The Primo Vascular System: Its Role in Cancer and Regeneration. *Springer Science + Business Media* pp 47-54
12. Yoo JS, et al., “Bonghan ducts as possible metastasis-paths of cancer.” J acupunct Meridian Stud 2:118-12312
13. Vodyanoy Vitaly, et al., “Evaluation of a New Vasculature by High Resolution Light Microscopy: Primo Vessel and Node”, *Quotative Biology*, arXiv:1608.04276, Aug, 2
14. Kim BH, “Kyungrak System and Sanal Theory. Medical Literature, Pyongyang, DPRK, 1965
15. Lee BC, et al., “Toward a Theory of the Primo Vascular System: A Hypothetical Circulatory System at the Subcellular Level”, *Evid Based Complement Alternat Med*. 2013; 2013: 961957.
16. Lee SJ, et al., “Adult stem cells from the hyaluronic acid-rich node and duct system differentiate into neuronal cells and repair brain injury” *Stem Cells Dev*. 2014 Dec 1; 23(23): 2831–2840.
17. Rai R, et al., “A Hyaluronic Acid-Rich Node and Duct System in Which Pluripotent Adult Stem Cells Circulate.”, *Stem Cells Dev*. 2015 Oct 1;24(19):2243-58

Chapter 6

Conclusion

Chapter 6

Acupuncture is based on a system of meridians, which is one of the primary methods of treatment from the history. This research work is a priceless heritage handed down by our ancestors. In current researches, a number of variety methods have been used to identify meridians and to explain them anatomically.

In this thesis, three issues in Primo Vascular System were investigated. They are the evidence of the existence of PVS, correspondence of superficial PVS to acupuncture meridian. These are a series of experiment was performed in which many questions are raised in the backing of Dr. Kim's theories and experiments, but I think everyone should consider the importance and necessity of these experiments. With understanding of modern scientific thinking and access to new technologies are also considering important issues of this study.

Here I present the morphological characteristics of PVS we discovered. In the first chapter, we found a novel PVS in the middle of the ventral abdominal wall as flowing duct connected to the OS-PVS. There are still many steps to go to visualize the whole network with an injection method. However, this work itself was very meaningful to show that the PVS can be traced by injecting nanoparticles in a PN for the first time. And during the investigation, we could add a good insight on why the PVS was not noticed or recognized in conventional histological analysis of the skin. Even we could detect the abundance of innate immune cells (MCs, etc.) in the PNs repeatedly. This suggests presence of the mast cells as a cytological criterion of the PN. As I described, the study of relation between mast cells in connection with the PVS and lymph system would be very beneficial for further investigation step.

Extend to the previous work; we decided to broaden the scope to research the ultrastructure of PV floating in a lymph vessel. Observing of the PVS floating in a lymphatic system was done by a few times. However, there

have been no studies on the ultrastructure of the entire cross section of a primo vessel with TEM. As I mentioned that, PVS can be found in anywhere in the body but we didn't know it would have same morphological features depending on the locations we found or it would be characterized by the finding location on related organs. But it turned out that detailed morphological features of PV were revealed and shown to be similar to another kind of the PV and at same time would make us to recognize the characteristic histological difference of the PV from the lymphatic vessel.

As many other research groups said that it is very hard to reproduce the results and even Dr. Kim's method was not fully presented in the articles. Owing to this situation, we became aware of the necessity of a new standard of developing method to identify the APs more easily. AP is another name for PN found beneath the epidermis and above muscular region. Its anatomical locations and sizes are key questions in addition to the traditional measurement method. For the answer to these questions, we became aware of necessity of the developing method to identify these precisely.

Many of studies so far focused on the matter of mast cell degranulation or dermal electrical impedance measurements to describe the APs; however, there are still many loopholes in current existing methods. As a way to supplement this, we investigated the whole transverse section of ventral skin and collected data. Based on the data, I chose to present the CV8, two KI 16 points in this article. From what we found, AP is a small and ellipse shaped structure, but due to the connective tissues surrounded to it, it was slightly difficult to distinguish from the adjacent tissues. This structure is surrounded by blood capillaries. The traditional cun measurement method was not applicable to assume a precise location of points as described in the book. Thus, we used the distribution of MCs at three acupoints to estimate the locations, sizes, and depths from the epidermis. Through this study, we could define that MCS and APs have a relation for sure but it can't be say that it is a sufficient condition to define the APs. Because the regions highly populated with MCs did not always coincide with conventionally designated APS

therefore for the further study, it would be better to investigate the distributions of MCs for other skin areas or pathological conditions in experiment animals to confirm what we found in this work.

As stated above, the medical significance of the PVS is still investigated but data have already been accumulated showing its possible role in immune system suggested by the many mast cells found around the location of the PV and PN. The technologies are further developed and applied in this field; it could offer a glimmer of hope on the physiological mechanism based upon oriental medicine theory. The modern scientific research in the PVS theory, which is an accumulation of rich therapeutic and prophylactic experiences, opens up the great possibilities of exploring a new sphere of medical sciences.

국문 초록

침술은 한국, 중국 및 일본에서 수천 년 동안 전해 내려오던 주요 의술이었지만 아직 침술의 기초 메커니즘은 명확하게 밝혀지지 않았다. 이전의 많은 연구들에서 여러 방법으로 경혈 및 혈 자리에 해당하는 곳의 해부학적 구조와 생리학적 기능을 규명하려고 노력하였으나 많은 어려움을 겪었고, 1960년 초에 최초로 김봉한 (Bong Han Kim)에 의해 처음으로 발견되어 이를 봉한 시스템으로 또 2012년부터는 프리모 시스템 (Primo Vascular System, PVS)으로 소개되었다. PVS는 혈관계 및 림프계와 함께 새로이 발견 된 세 번째 순환계로 대중들에게 소개되고 있다.

건강 관련 분야에서 이 새로운 3 순환계의 잠재적 중요성에도 불구하고, 이 분야의 연구는 빛을 보지 못한 채 많은 연구자들에게 오랫동안 외면되어 왔다. 최근에서야 경락·경혈을 연구하는 연구자들에 의해 이 시스템의 물리적, 생리학적 특이성 관련 이론 및 방법론들에 관한 연구방법들이 다양하게 제시되고 있다. 이에 다양한 관련 연구들이 계속적으로 수행되고 있는 상황이지만 아직도 침구학의 복잡한 기작에 관해서는 충분히 밝혀지지 않고 있는 실정이다. 심지어 김봉한의 이론과 가설에 따라 수행된 실험 결과에서 조차도 그 신뢰성을 둘러싼 많은 논란들이 현재까지 이슈화 되고 있다.

따라서 이 박사논문에서는 PVS 시스템에서 제시된 이론들 중 세가지 파트로 나누어 실험을 통하여 이를 증명하고자 하였다. 이 세가지 실험 목표는 각각 PVS의 해부학적 특징들을 증명하고, 이를 바탕으로 한 기전의 이해를 돕기 위한 새로운 분석 방법을 제시하고자 한 것이 최종 목표였다.

그 첫 번째에서는 항상 PVS란 단어가 나오면 쟁점이 되는 두 가지 사항에 관해서 증명하고자 하였다. PVS는 순환계의 한 종류로서, 이를 증명하기 위해서는 첫째가 액체가 프리모 관 내에서 흐른다는 것을 보여 주는 것이 중요하고, 두번째가 왜 기존에 사용되는 조직학적 분석방법으로 일반 동물 조직에서 PVS가 쉽게 구분 및 관찰이 되지 않는 점에 관해 설명 하는 것이다. 이에 대한 해답을 얻기 위해서 우리는 프리모 노드에 형광나노입자 (FNPs)를 주입하고, 복 벽에 위치한 linea alba와 평행한 지방 조직 내부에 위치한 프리모 관을 찾아 이를 따라 흐르는 형광나노입자 (50nm) 들을 추적하는 시도를 하였다.

이전 프리모 실험에는 주로 알시안 블루 염색 염료 (Alcian blue)를 프리모 노드에 주입 후 일정 시간이 지난 후, 관 내에 염색된 프리모 관을 가시화하여 관찰하는 실험을 주로 하였다면, 이번 실험은 형광나노입자가 PVS의 하위 시스템으로 흐르는 것을 추적하여 흐른다는 것을 보이는 것이 가장 중요한 목표이자 이 실험의 가장 큰 성과라 할 수 있을 것이다. 이는 PVS에 흐를 수 있는 관이 존재함을 보여주는 자료가 될 뿐 아니라 동시에 순환계가 갖춰야 하는 조건들을 갖추었다는 것을 증명할 수 있는 첫 번째 결과였기에 그 의미가 크다고 할 수 있다. 또한 기존에 실행 되고 있는 조직학적 분석 방법으로 PVS를 왜 쉽게 관찰 할 수 없는지 또 주변 조직과 구별이 어려운지에 대한 힌트를 얻을 수 있었다는 것이다.

앞선 연구 결과들 에서 항상 PVS 후속연구의 중요성들이 언급되었는데, 그 중 한가지가 관 내 떠있는 프리모 관 (PV)의 자세한 미세구조를 분석, 이를 몸의 다른 부분에 존재하는 프리모 관과 비교하여 이들의 특성 및 유사성에 관한 분석을 하는 것이었고 또 다른 한가지는 피부에 위치한 표층봉한소체 (skin PVS)를 찾을 수 있는 방법 제시에 관한 것이었다.

이에 우리는 투과 전자 현미경 (TEM)으로 림프관 내부의 떠있는 프리모관 (PV)의 형태학적 특징들을 일차적으로 자세히 조사한 뒤, 이를 장기표면에서 발견한 PV의 결과와 비교 분석하였다. 이 결과를 통해 알 수 있듯이 다른 부분에서 발견된 PV들의 하위 시스템들이라 할지라도 부분의 특성화 되어 있다기 보다 기본 특성들은 매우 유사함을 확인할 수 있었다.

마지막으로 이 논문에서는 피부에 위치하고 있는 프리모 노드를 찾는 것을 최종 목표로, 같을 것이라고 추정되는 피부조직에 위치한 혈 자리 (APs)에 관해 과학적 근거에 바탕을 둔 정확한 해부학적 정보를 제시 할 수 있는 방법론에 관한 연구를 진행하는 것에 목표를 두었다. 현재까지 다른 연구자들에 의해 발표된 결과들은 전통적 측정 방법을 이용, 동물의 몸에서 혈 자리를 정한 뒤, 추정되는 혈 자리와 주변의 비 혈 자리위치를 비교, 이의 방법으로 비만세포 수 비교와 전기적 특성을 바탕으로 분류하는데 초점이 맞춰져 있었다.

하지만 이번에 진행된 실험에서는 기존에 많이 사용되는 방법인 한 부분의 혈 자리와 비 혈 자리의 비만세포의 밀도와 수에 대한 선택적 조사가 아닌 CV 8을 포함한 배 쪽 전체 피부 조직을 면적을 크게 절개해서, 혈 자리와 비 혈 자리를 미리 추정하지 않은 채, 비만세포의 수와 밀도 등을 전체적으로 먼저 조사 후, 이 결과를 바탕으로 기존에 사용되는 전통적 춘 측정 방법으로 혈 자리라고 생각되는 곳과 비교 분석하여 피부에 위치한 피부 프리모 노드를 정확히 추정할 수 있는 방법 도출에 관한 연구를 수행 하는 것이었다. 현재까지 발표된 많은 선행연구 결과에서는 혈 자리와 비만세포의 관련성에 대해서는 설명을 하였지만 왜 혈 자리에 유독 비만세포의

증가가 있는지, 또 왜 혈 자리가 아닌 곳에도 비만세포가 존재 하는 것인지에 대해서는 여전히 설명하지 못하고 있는 상황이다.

이에 우리 팀은 마우스의 피부 조직에서 한 부분만이 아닌 복부 피부 조직에 비만세포의 염색을 위해 톨루이딘 블루 염색을 진행한 뒤 배꼽을 포함한 부위의 횡단면의 면적을 크게 절개 후, 비만세포의 분포도와 밀도를 조사, 이를 피부 층에 위치한 혈 자리 (skin PN로 추정되는)의 위치, 크기 및 깊이를 추론 하는 방법에 사용하였다. 이러한 유형의 추정은 이번 실험을 통해서 처음 제시되었고, 이번의 획득한 실험 결과는 앞으로 진행될 표층 봉한 소체에 관한 후속 연구에 중요한 자료로 쓰일 수 있으리라 생각된다. 또한 이 실험 결과에서 보여주었듯 현재까지 많이 쓰여지고 있는 혈 자리 측정지표인 비만세포의 밀도 및 수는 이를 명명하는 한 요소로는 사용할 수 있음을 알 수 있었으나 이 외에도 고려해야 할 중요한 요소들이 더 있을 수 있음을 확인할 수 있는 것이었다. 또한 사람에게 적용되는 전통적 위치측정 방법은 실험동물에 적용 시 많은 에러가 생길 수 있음을 알 수 있었다.

하지만 동시에 우리가 간과할 수 없는 부분은 혈 자리 주변에 많이 나타나는 비만세포에 관해서다. 비만세포는 우리 몸의 면역체계와 밀접한 관련을 가지고 있기에, 질병 케이스에서 혈 자리 (프리모 노드)를 정확하게 컨트롤 함으로써 생기는 면역체계의 기전을 밝히는 데 중요한 밑거름 역할을 할 수 있다는 것이기 때문이다. 이에 피부 혈 자리의 서브 밀리미터 정밀도를 밝히는 해부학적 연구는 표층 봉한 소체 (S-PN) 대한 정확한 지식 전달 및 이에 관련된 세포학적 특성에 관한 정보를 얻을 수 있는 중요한 부분이라고 할 수 있다.

주요어: 프리모시스템, 비만세포, 톨루이딘 블루, 혈 자리, 경락,
면역시스템, 전자현미경, 형태학적 구조, 표층봉한소체

학번: 2014-30808